Negligible microbial matground influence on pre-vegetation river functioning: evidence from the Ediacaran-Lower Cambrian Series Rouge, France

William J. McMahon[1]*, Neil S. Davies[1], David J. Went[2]

[1] *Department of Earth Sciences, University of Cambridge, Downing Street, Cambridge CB2 3EQ.*

[2]*Arunside Limited, Silver Birches, Fox Hill Village, Haywards Heath, RH16 4QZ*

*corresponding author: wjm39@cam.ac.uk

Abstract

The pre-Silurian alluvial rock record is dominated by accumulations of laterally-extensive, sheet-like sandstone strata with minimal mudrock; a depositional style frequently explained as representing fluvial processes particular to "pre-vegetation" Earth. While the sedimentological and geomorphological influence of Palaeozoic embryophytes and other higher vegetation has been commonly inferred, the influence of the non-marine microbial matgrounds that preceded them has been less well studied. The ?Ediacaran-Cambrian Series Rouge of northern France and the Channel Islands is a rare example of a predominantly alluvial succession which exhibits both pre-vegetation sedimentary motifs and evidence for the existence of terrestrial microbial mats. The latter include likely microbial sedimentary surface textures, the enigmatic matground "pseudofossils" *Aristophycus* and *Arumberia*, and probable mat fragments and mat-related microtextures preserved in argillaceous sediment. The sedimentological characteristics of the Series Rouge are described and analysed in order to assess the role of microbial influences on pre-vegetation alluvial systems. Near ubiquitously trough-cross bedded sheet-braided facies, with rarely preserved channel-forms, indicate that alluvial sedimentation was dominated by in-channel dune migration, and depositional-strike exposures reveal the periodic downstream migration of complex bar-forms. Lateral accretion elements and minor discontinuous lenses of more argillaceous material are locally present. Thus, despite the evidence for matgrounds, sedimentary architecture was essentially 'abiotic'. Using this evidence from the Series Rouge, we argue that the surficial cohesion provided by matgrounds did not exceed thresholds for

reworking by hydrodynamic processes thus having little or no effect on their preserved sedimentary architecture.

Keywords: Precambrian, fluvial, alluvial, architectural analysis, MISS, biofilm

1. Biotic influences on pre-vegetation river systems

In modern rivers, vegetation strongly influences fluvial styles and processes through the moderation of weathering rates, sediment supply, and the promotion of increased channel stability and surface roughness (e.g., Schumm, 1968; Thornes, 1990; Tal and Paola, 2007; Moor et al., 2017). In contrast, ancient rivers that operated prior to the existence of land plants were exempt from such influences. By combining these understandings with physical evidence from the geological record it has been demonstrated that the facies and architecture of Palaeozoic alluvium exhibit a stepwise evolution of characteristics, stratigraphically aligned to evolutionary advances in terrestrial vegetation (Cotter, 1978; Davies and Gibling, 2010a; Davies et al., 2011; Gibling et al., 2014). Complex heterolithic architectures are far more common in rocks of late Silurian or younger age, reflecting how the evolution of rooted tracheophytes provided novel means of floodplain stabilization and the retention and production of finer sediment (e.g., Algeo and Scheckler, 1998; Gensel et al., 2001; Hillier et al., 2008). In contrast, alluvial sedimentary rocks of pre-Silurian age exhibit a distinct suite of 'pre-vegetation' characteristics (Table 1).

Despite the distinct nature of pre-vegetation alluvium, it is now recognised that the landscapes in which such deposits were lain down were not wholly abiotic. Prior to their 'greening' by embryophytes and other higher land plants, Earth's non-marine environments likely hosted abundant microbial mats and biofilms (e.g., Horodyski and Knauth, 1994; Noffke, 2010; Wellman & Strother, 2015). In light of this, an increasing number of recent studies have postulated that microbiota may have influenced geomorphic stability and processes in Precambrian and early Palaeozoic rivers (e.g., Medaris et al., 2003; Sarkar et al., 2005; Eriksson et al., 2009; Bose et al., 2012; Petrov, 2014, 2015; Ielpi, 2016; Santos and Owen, 2016). These assertions were primarily made by combining (1) the

recognition that mats would have been present in the pre-vegetation realm, with (2) reference to observations of microbial influences on sedimentary processes in modern environments or laboratory experiments. Such modern observations include demonstrations of how extracellular polymeric substances (EPS), secreted by microbiota, alter the thresholds of sediment entrainment, transport and deposition (e.g., Vandevivere and Baveye, 1992; Tolhurst et al., 2002; Friend et al., 2008; Malarkey et al., 2015), or observations of how microbial mats prolong substrate stabilization under moving fluids, prior to their catastrophic failure (Krumbein et al., 1994; Hagadorn and McDowell, 2012; Vignaga et al., 2013).

Understanding exactly how a microbial influence may have been exerted on pre-vegetation rivers is currently hampered by a paucity of studies that provide direct supporting physical evidence from the geological record. In part this is because Precambrian and early Palaeozoic alluvial strata only rarely preserve fossil evidence for the presence of microbial mats during deposition (Schieber, 1999; Noffke et al., 2001; Davies and Gibling, 2010; Davies et al., 2011, 2016). Our survey of pre-vegetation fluvial units includes only 9 formations which simultaneously host evidence for microbial life (Prave, 2002; Parizot et al., 2005; Yeo et al., 2007; Rasmussen et al., 2009; Sheldon, 2012; Beraldi-Campesi et al., 2014; Wilmeth et al., 2014; Petrov, 2014, 2015). Even fewer studies have directly used sedimentary geological evidence to support assertions of how these ancient mats may have influenced fluvial processes.

Petrov (2015) interpreted a microbial mat influence on fluvial landscapes in the 1.58 Ga Mukun Basin of Russia, but the sedimentary architecture of the associated strata was not detailed, and many of the 'microbial-related structures' within the fluvial facies are more parsimoniously interpreted as abiotic features (adhesion marks, ladder ripples, accretionary dunes and soft sediment deformation; see Davies et al., 2016). Santos and Owen (2016) postulated that the development and preservation of Precambrian fine-grained meandering rivers could have been promoted by microbial mats. This was supported by the presence of one 8 metre-thick fine-grained interval (including heterolithic lateral accretion) within a 3000 metre-thick succession of otherwise sheet-braided sandstones of the Neoproterozoic Applecross Formation in Scotland. Santos and Owen (2016) noted that no physical

evidence for microbial mats is present anywhere in the Applecross Formation. Medaris et al., (2003) used petrological evidence from the Palaeoproterozoic Baraboo Quartzite (northern USA) to infer a microbial influence on pre-vegetation alluvium. They suggested that the supermature nature of these fluvial sandstones may have been promoted by intense chemical weathering of interfluves, stabilized for prolonged periods by hypothesised microbial soil crusts.

With these notable exceptions, most other reports of a microbial influence on Precambrian sedimentation are wholly hypothetical (e.g., Bose et al., 2012) and there is thus a knowledge gap arising from a scarcity of studies which directly use sedimentary geological evidence to support or contend assertions of microbial influence on pre-vegetation rivers. The present study, attempts to redress this with reference to the Ediacaran-Cambrian "Series Rouge" of northwest France, which provides an excellent opportunity to study the interactions between matgrounds, pre-vegetation river systems, and preserved alluvial architecture. The Series Rouge is well-suited for such a purpose in that it contains both well-exposed outcrop of alluvial architecture, in addition to multiple lines of evidence for former microbial mat colonies. This paper is organised as follows: (i) an introduction to the geological context of the Series Rouge; (ii) an analysis of the lines of evidence for microbial life within the succession; (iii) an analysis of the sedimentary architecture and facies of the succession; and (iv) a discussion of how microbial life (evidenced in Section 3) influenced the sedimentary characteristics of the Series Rouge (evidenced in Section 4).

2. Geological Context of the Series Rouge

Neoproterozoic and lower Palaeozoic red bed successions, deposited during the terminal stages of the Cadomian Orogeny, crop out across northwest France and the Channel Islands (Renouf, 1974; D'Lemos et al., 1990; Went and Andrews, 1990). Stratigraphic nomenclature of the red beds is confused, in part due to the scattered nature of outcrop in isolated geological inliers and outliers, on islands, and in part due to the cross-border spread of outcrop in northern France and on the UK Channel Islands of Alderney and Jersey (Fig. 1). The stratigraphic terminology used for the French outcrops is localized to each individual outcrop belt, but they are informally grouped as the "Séries

Rouges du Golfe Normano-Breton". The British Geological Survey recognises the Alderney Sandstone and Rozel Conglomerate (Jersey) as discrete mapping units, but does not relate them to one another or to the French outcrops. Here we use the term 'Series Rouge' to group the geographically-proximal red-bed outcrop areas on both the Channel Islands and French mainland. Formal stratigraphic correlation is presently impossible due to a lack of reliably dated markers, but we use the term to refer to all the unfossiliferous sandstones, conglomerates, and mudstones that share a common basal unconformity above deformed Neoproterozoic shales and volcanic rocks (the Brioverian Series) or plutonic igneous complexes in the region (summarised in Fig. 2). The precise age of the Series Rouge is still subject to discussion. Red-bed sequences in Normandy unambiguously underlie Cambrian Stage 3 (521 – 514 Ma) limestones (dated by the presence of the trilobite *Bigotina* (Pillola, 1993)) and pre-trilobite marine siliciclastics from Cambrian Stage 2 (529 – 521 Ma). The red beds in northern Brittany are less well constrained stratigraphically, but are lithologically similar to the Normandy red beds. The French Geological Survey considers them Early Ordovician, on the basis of radiometric data obtained from the intercalated Plourivo-Plouezec andesitic volcanics (Auvray et al., 1980). However, field relationships exhibited by the andesites indicate the radiometric date is undiagnostic (Went, 2016) and palaeogeographic considerations render an Early Ordovician age implausible. Palaeocurrent data demonstrate that alluvial strata of the Series Rouge were derived from the west ($\theta = 84°$; $n = 431$), but there is no potential Early Ordovician source for such sediments in this direction, where well-dated marine shelf sediments (the Gres Armoricain) were being lain down during this interval (Paris et al., 1999; Dabard et al., 2007, 2009). The weight of evidence thus suggests that the Series Rouge were deposited between the latest Ediacaran and earliest Cambrian – although even if they were Early Ordovician they would still unambiguously represent pre-vegetation strata. Deposits included in the Series Rouge cover a range of depositional environments (Fig. 2). At Goëlo, the lower Port Lazo Formation passes upwards from alluvial fan-alluvial plain deposition into a subtidal setting, before transitioning into braided fluvial deposition of the Roche Jagu Formation (Went, 2016). At Baie de St-Brieuc, with the exception of a 30 m interval of mature marine quartzites representing nearshore marine environments (Went, 2013), braided alluvium predominates. Alluvial fan conglomerates dominate the stratigraphy on Jersey (Went et al., 1988; Went, 2005), whereas

coeval sandy alluvium (and subordinate marine sandstone) comprises the Alderney succession (Todd and Went, 1991; Ielpi and Ghinassi, 2016). Couville Formation conglomerates and arkoses most likely have an alluvial origin (Doré, 1994).

3. Evidence for microbial life in the Series Rouge

A suite of circumstantial evidence for microbial life in the Series Rouge consists of petrographic evidence, the presence of sedimentary surface textures, and two enigmatic 'pseudofossils', *Aristophycus* and *Arumberia*. The following sections critically discuss these lines of evidence from the Fréhel and Port Lazo Formations (Fig. 2), combined with previously reported evidence from the Rozel Conglomerate in Jersey (Bland, 1984).

3.1. Petrographic Evidence

Positive identification of microbial mat features from petrographic thin sections can be challenging because they share similarities with other laminated structures produced by purely physical means (e.g., differential compaction of anisotropic sediment (Schieber, 1999)). Despite this, circumstantial petrographic evidence for the presence of matgrounds during deposition exists within fine-grained alluvial sedimentary rocks of the Fréhel Formation, which occur either as discontinuous layers, or as red or white blocky intraformational mud clasts in sandstones. Such mudstones and siltstones contribute <1% of the thickness of the formation, yet, where these have been sampled, they always contain features in thin sections that may be characteristic of former microbial mats, including abundant detrital mica and probable carbonaceous material.

Detrital biotite mica is a near ubiquitous component of both red and white mudstones of the Fréhel Formation (Fig. 3). The biotite micas are most commonly weathered and degraded, and present as aligned, near-isotropic (due to alteration to ferric oxide), <0.5 mm flakes with little or no observable cleavage (Fig. 3A). The weathered biotite contrasts with locally-present fresher biotite, which exhibits a pale green colour and characteristic cleavage planes (Fig. 3B). Mica flakes vary in abundance between sampled mudstones, either displaying an even distribution across the sample (Fig. 3A), or occurring as discrete, dense layers in which mica flakes surround grains in an anastomosing fashion

(Fig. 3C, 3D). The segregation of mica results from settling velocities that are much lower than for quartz grains of similar size (Doyle et al., 1983). For this reason they tend to float and accumulate preferentially in quiet water settings along with silts and clays. Such low energy fluvial subenvironments (such as floodplain ponds) are most suited to matground development. Here, mica may avoided resuspension and become trapped and bound in these environments due to the secretion of EPS by microbial matgrounds, termed the 'fly paper effect' (e.g., Gerdes and Krumbein, 1987; Schieber, 1999, 2004; Schieber et al., 2007). The association between densely packed mica and microbial matgrounds is further suggested by abrupt, convex-upward features within mica layers (Fig. 3B, 3C). This morphology is frequently described as 'wavy-crinkly' (e.g., Gerdes and Krumbein, 1987; Schieber, 1999, 2004) and is sometimes cited as evidence for microbial mats where present in the sedimentary record (Schieber, 1999; Sur et al., 2006; Deb et al., 2007; Samanta et al., 2011), on the basis that modern microbial mat laminae regularly display a similar morphology (Horodyski et al., 1977; Krumbein and Cohen, 1977).

Fragments of possible carbonaceous material are also present in petrographic thin sections of the Fréhel Formation, and may represent comminuted microbial mats. Carbonaceous material is predominantly isotropic (Fig. 3E, 3F, 3G). Carbonaceous material occurs in two ways: (1) as elongate laminae, potentially representing *in situ* matgrounds (Fig. 3E); or, (2) more commonly, as <0.25 mm long stringers, potentially representing reworked fragments of matgrounds (Fig. 3F). In instances where the material is present as laminae, these usually occur in isolation and are separated by up to 0.5 mm of background sediment (Fig. 3E). Carbonaceous laminae are particularly common in thin sections made from intraformational mud clasts, where they exhibit discrete internal laminae that may have strengthened the clasts against physical attrition (Fig. 3G). In contrast, stringers occur in isolation, with evidence for internal cohesion and rigidity, such that they were able to bend and fold prior to and during deposition; some carbonaceous stringers are differentially compacted around isolated quartz grains (Fig. 3F) (Schieber et al., 2010).

Caution is required in distinguishing carbonaceous flakes from degraded biotite. Detrital biotite tends to fray at its margins, break along cleavage planes and become isotropic when altered to iron oxide

187 (Fig. 3H) (Fordham, 1990). In the Fréhel Formation, carbonaceous stringers may be distinguished
188 from detrital biotites by (1) lower relief (Fig. 3A v Fig. 3E), (2) more continuous laminae (Fig. 3E),
189 and (3) a lack of evidence for cleavage planes.

190 **3.2. Sedimentary Surface Textures**

191 Mudrocks within the braided alluvium of the Fréhel Formation and the probably marine-influenced
192 alluvial plain deposits of the Port Lazo Formation display a variety of sedimentary surface textures.
193 Some of these may be related to microbial processes and would thus be referred to as referred to as
194 'microbially induced sedimentary structures' or MISS (sensu Noffke et al., 2001). Obtaining
195 conclusive proof of a microbial origin for a particular sedimentary surface texture in the ancient
196 record during initial field observation can be problematic, as many abiotic mechanisms can produce
197 MISS-like textures (Davies et al., 2016). As a result, each surface texture described below is assigned
198 a sedimentary surface texture category, indicating the degree of certainty of a microbial formation
199 mechanism (Davies et al., 2016). Category B are definitively biotic (microbial) and category A are
200 definitively abiotic. Category Ba is assigned for structures with evidence for a biotic origin, but an
201 abiotic origin cannot be ruled out (Ab for the converse situation). Surface textures with a plausible
202 biotic origin, but where there is no clear evidence are classed ab.

203 *3.2.1. Transverse wrinkles* (**ab**); (Fréhel and Port Lazo Formations): Wrinkles (*sensu* Davies et al.,
204 2016) may have abiotic or microbial origins. Within the Fréhel Formation, wrinkles are irregular,
205 broadly subparallel and occur superimposed on irregular mm-relief topographic highs that are spaced
206 approximately 1 cm apart (Fig. 4A). The long axes of these structures trend E-W, perpendicular to the
207 predominant eastward flow orientation observed from cross-strata and rippled surfaces. Within the
208 Port Lazo Formation, wrinkles display strong, parallel alignment, have mm-scale spacing and are
209 highly discontinuous (individual ridges are predominantly < 2.5 cm long) (Fig. 4B). The strike lines
210 are highly variable (unlike those in the Fréhel Formation). Individual ridges are spaced 1 – 1.4 mm
211 apart and have heights < 0.5 mm.

3.2.2. 'Bubble' texture (**ab**); (Fréhel Formation): Multiple, circular, epirelief 'bubbles' are no more than 1 mm in diameter and have a patchy distribution across the surface, but when present occur as densely spaced clusters (Fig. 4C). They differ to epirelief bulges (Section 3.2.3) by being smaller and more densely packed. The structures have a near uniform size distribution and rarely overlap. Similar textures may be formed by a respiring matground (Noffke et al., 1996), though abiotic origins cannot be ruled out. For example, within modern intertidal sediments, air-escape bubbles frequently form near the strandline during falling tide, as well as beneath clay veneers (De Boer, 1979; Davies et al., 2016).

3.2.3. Epirelief bulges (**Ba**); (Fréhel Formation): Simple isolated bulges occur on numerous bedding planes (Fig. 4D). They occur as sub-circular domes preserved in positive epirelief, typically 2 - 4 mm in diameter. The formation of similar bulges has been previously attributed to gas release from within a microbial surface (Dornbos et al., 2007; Gerdes, 2007). Oxygen-rich bubbles may remain stable for weeks or months if they are not disturbed, permitting them to become enmeshed by filamentous cyanobacteria (if present), and potentially preserved (Bosak et al., 2010).

3.2.4. Ruptured domes (**Ba**) (Port Lazo Formation): Ruptured domes occur alongside *Arumberia* (Section 3.3.2) on desiccated surfaces within in the Port Lazo Formation lower Member. These are discoidal ring shaped bulges no more than 30 mm in diameter and 3 mm in height. Each dome contains a central depression (Fig. 4E). Shape varies from circular to fairly elongate. Domes are typically clustered. Ruptured domes are probably the result of burst bubbles that could occur either within a matground or clay veneer.

3.2.5. 'Elephant skin texture' (**Ba**); (Port Lazo Formation): The term 'elephant skin texture' has become a bucket term for many different textures, having been consistently misapplied in recent years (Davies et al., 2016), but the Port Lazo Upper Member contains infrequent examples of the texture that match the original description of Runnegar and Fedonkin (1992). The texture consists of a tight network of reticulate ridges (Fig. 4F). Width of individual polygons within the network is < 5 mm. Orientation of individual ridges are highly irregular. The origin of the structure is uncertain, but it has

been described from multiple microbial matground facies, particularly in Ediacaran strata (e.g., Gehling, 1999; Steiner and Reitner, 2001).

3.2.6. Curved shrinkage cracks (**ab**) (Port Lazo Formation): Curved cracks with tapering edges are preserved in the Port Lazo Formation (upper Member only) (Fig. 4G). It has been proposed that such cracks require a microbial binding of surface sediment to form (Gerdes, 2007; Harazim et al., 2013), though abiotic explanations also exist (Allen, 1982; Astin and Rogers, 1991; Pratt, 1998).

3.2.7. Reticulate markings (**Ba**) (Port Lazo Formation): Reticulate markings are occasionally associated with *Arumberia* in the Port Lazo Formation (Fig. 4H). Such markings may develop on a microbial mat when filamentous bacteria glide, collide and amalgamate (Shepard and Sumner, 2010), or from the tangling of algal filaments (Davies et al., 2016).

3.2.8. Assessing microbial origins for the sedimentary surface textures

Interpretations of microbial origins for these sedimentary surface textures are made with a caveat of reasonable uncertainty. The majority of the surface textures described above can be classified as 'ab' (Davies et al., 2016) as there is no unambiguous evidence to support either a definite biotic or abiotic formation mechanism. However, the high abundance and diversity of enigmatic ab and Ba sedimentary surface textures within close spatial proximity may lend support to a microbial origin for at least some of the textures because (1) microbial mats broaden the potential range of interaction between physico-chemical processes and a sedimentary surface; (2) and can be interred at different stages of their morphological development (Schieber, 1999; Gehling and Droser, 2009; Davies et al., 2016, 2017).

3.3 "Pseudofossils"

3.3.1. *Aristophycus*

Two examples of the enigmatic branching structure *Aristophycus* (Osgood, 1970; Davies et al., 2016) occur on a single bedding plane of very coarse-grained, trough cross-stratified alluvial sandstone (Fig.

5A), 50 metres above the base of the Fréhel Formation (Fig. 2). The sediment immediately overlying the structures is considerably finer (fine to medium sand) and more micaceous (Fig. 5E). Petrographic evidence demonstrates that the composition of the raised *Aristophycus* structure is predominantly quartz and feldspar (Fig. 5B), but the sandstone underlying the branching structure hosts densely packed detrital mica flakes (Fig.5D). Detrital mica is less common within the host sandstone at greater distances, both laterally (Fig. 5C) and vertically (Fig. 5D) from the *Aristophycus* structures.

Three hypotheses for *Aristophycus* formation have been proposed: (i) Expulsion of pore water through burrow cavities (Seilacher, 1982); (ii) Dewatering of unconsolidated sands beneath an impermeable clay seal (Knaust and Hauschke, 2004) (iii) The movement of fluidized sediment trapped beneath an impermeable microbial mat (Seilacher, 2007; Kumar and Ahmad, 2014). The sandstones of the Fréhel Formation pre-date terrestrial burrows so the first hypothesis can be rejected in this instance. The two described examples of *Aristophycus* are interpreted as dewatering structures incorporating elements of hypotheses ii and iii above. Expelled pore fluid appears to have been unable to migrate vertically upwards through the micaceous sandstone and instead moved laterally from a point source in the very coarse sandstone along a conduit before dissipating into a small number of breach points in the overlying bed. Thus, *Aristophycus* is interpreted to mark the route of water escape through this locally heterogeneous system. The isolated stratigraphic occurrence of the structure is explained by the fact that the bulk of the Fréhel Formation records more high energy fluvial deposition, and is unsuited to the formation of *Aristophycus* by virtue of being homogenous with regard to permeability. The role of mats in the origin is inferred from the densely packed detrital mica immediately underlying *Aristophycus* (Fig. 5D) (see Section 3.1).

3.3.2. *Arumberia*

Multiple red or reduced drab mudstones within the Port Lazo Formation contain examples of the enigmatic sedimentary surface texture, *Arumberia* (Fig. 6). The most prominent *Arumberia* location occurs near the top of the Lower Member of the Port Lazo Formation at Bréhec (Fig. 2), where multiple examples are spread extensively across a 300 m^2 desiccated surface within a heterolithic mottled red bed succession that records probable tidally influenced alluvial plain facies (Went, 2016).

Previous reports have also noted *Arumberia* within basal red mudstones of the Rozel Conglomerate at Tête des Hougues, Jersey and in red mudstones overlying the Erquy Conglomerate at Pointe des Trois Pierres, Brittany (Bland, 1984).

Arumberia was originally interpreted as an Ediacaran metazoan (Glaessner & Walter, 1975) before being reinterpreted as a physical sedimentary structure (Brasier, 1979), and is now more commonly described as a microbially-induced sedimentary structure (McIlroy & Walter, 1997). It comprises a series of parallel or sub-parallel, occasionally bifurcating rugae (< 1 mm relief), spaced c. 1 - 3 mm from one another (Fig. 6A, 6B). In the vast majority of instances, the rugae are seen as parallel lines, often in association with small 'spheroid impressions' (Bland, 1984), 0.5-1.5 mm in diameter and < 1 mm in relief (Fig. 6C). Petrographic thin sections demonstrate that carbonaceous laminae occur in close association with the *Arumberia* (Fig. 6D, 6E). The structure remains enigmatic, but its tight global stratigraphic range between 630 - 520 Ma (Bland, 1984), association with carbonaceous laminae, desiccated nature within subaerially-exposed facies, and morphological complexity suggest that it likely represents a preserved fossilized matground organism (Kolesnikov et al., 2012; Davies et al., 2016).

3.4. Microbial Landscapes of the Series Rouge

With the possible exception of *Arumberia*, none of the characteristics described in the above sections are definitive proof of microbial matgrounds, when taken in isolation. However, taken together, the co-occurrence of a variety of lines of circumstantial evidence, including petrographic signals, sedimentary surface textures, and discrete pseudofossils, lend support to the contention that the depositional environments of the Series Rouge were colonized by matgrounds. There is a strong facies-dependency to these signatures. Within braided alluvial facies (Fréhel Formation), evidence for matgrounds is restricted to more quiescent sub-environments, rather than higher energy sandy channels. In coastal alluvial plain facies (Port Lazo Formation), a variety of sedimentary surface textures, *Arumberia*, and petrographic signatures all occur in close-proximity within desiccated, subaerially exposed mudstones. Thus it appears that rivers operating in the Series Rouge depositional

environments would have had the potential to interact with microbial mats in both quiescent parts of their channel belts, and within their distal coastal reaches. The effect that these mats had on hydrodynamic processes is assessed below through study of the sedimentary architecture of the Series Rouge alluvium.

4. Sedimentary Characterisitcs of the Fréhel Formation

Detailed accounts of the sedimentary facies of the Series Rouge have previously been published and are summarised in Figure 2 (Doré, 1972; Todd and Went, 1991; Went and Andrews, 1991; Went et al., 1988; Went, 2005, 2013, 2016) but the sedimentary architecture has been less comprehensively studied (Ielpi and Ghinassi, 2016). Detailed evaluation of sedimentary architecture requires high quality, extensive exposures. The most suitable exposures in the Series Rouge occur in the Fréhel Formation.

The Fréhel Formation is characterised by repetitive stacked 0.2 - 1.0 metre thick cosets of trough cross-stratified sandstone, separated by erosional bounding surfaces (Fig. 7, Fig. 8A). The spacing between bounding surfaces decreases up through the formation concomitant with a decrease in average cross-set size. Conglomerates are common toward the base of the formation, but higher up the section they are limited to laterally discontinuous lenses or layers overlying down-flow dipping bar-form reactivation surfaces (Fig. 8B). Fine argillaceous sandstone and mudstone are scarce, restricted to very thin, discontinuous lenses and contributes <1% of total thickness. Palaeocurrents display a strongly unimodal eastwards palaeoflow direction (θ = 84°; n = 431; variance = 021° - 165°), consistent with previous studies (Went and Andrews, 1991).

4.1. Architectural Analysis of the Fréhel Formation

Coastal and quarry exposures of the Fréhel Formation permitted analysis of: (1) the dimensions, geometry and composition of constituent sediment bodies; (2) stacking patterns and lateral relationships from depositional-strike successions (perpendicular to palaeoflow), where a greater quantity of accretion macroforms were readily identifiable; (3) local downstream variation from depositional-dip successions (parallel to palaeoflow), which were better suited for revealing details of

lateral terminations and stacking patterns of individual bar-forms, channel-fills, and inclined lateral accretion surfaces.

Photomosaics of laterally-extensive strata were constructed during a reconnaissance visit and later used in the field so that beds could be accurately traced and locations of palaeoflow measurements and architectural elements precisely recorded, permitting a three-dimensional reconstruction of alluvial deposits (Allen, 1983; Miall, 1985, 1996; Long, 2006, 2011). Within the most extensive exposures, coset boundaries were seen to change in prominence laterally, passing into boundaries separating individual sand-bodies. In outcrop, such transitions can be picked out by variable weathering expressions of the bounding surface, and arise because larger bar-forms can separate into numerous smaller bars down-section (Allen, 1983). It has been suggested that annotation of bounding surfaces should leave no 'hanging lines' (Miall, 1996), but as the lateral transitions in these instances reflect original depositional processes, connecting lines is considered potentially misleading.

The cliff sections provide good lateral exposure of sedimentary architecture, but often at the expense of vertical access. However, coastal outcrops at Pointe aux Chèvre (Fig. 1) permitted detailed study of a c. 49 m thick vertical succession. The stepped nature of the exposure meant that architectural elements could still be accurately mapped laterally. Data collection was repeated for multiple vertically-stacked bar-forms, giving an indication of the temporal evolution of fluvial style.

4.1.1. Observed Architectural Elements vs. Interpreted Architectural Elements

Subdividing ancient alluvium into architectural elements permits the interpretation of past fluvial processes (Miall 1985). Such elements, within the Series Rouge, include sandy-bedforms (SB), downstream accretion (DA), downstream-lateral accretion (DLA), lateral accretion (LA), upstream accretion (UA), Fines (F) and Channels (CH) (e.g., Miall, 1985; Long, 2011) (Fig. 9). Whilst sound in theory, the practical application of this in natural rock outcrops has limitations because confident differentiation of bar-forms and channel-fills requires large, clearly-weathered three-dimensional exposures that are not always available. For example, the term '*accretion macroform*' encompasses all elements where cross-bed sets/cosets are genetically related to their underlying surface (e.g., DA, DLA, LA, UA elements (Fig. 9)). Conversely, the distinguishing characteristic of sandy-bedforms

(SB) is that they are not genetically related to their underlying surfaces (Miall, 1985). However accurately distinguishing SB from low sinuosity accretion macroforms (DA, DLA) can only be achieved where there is both good outcrop quality and orientation in relation to flow direction. Depending on the balance of depositional-dip/-strike exposures in an outcrop belt, exposure orientation can impose an observation bias on any census of architectural elements within a succession. A further discordance between theoretical and practical architectural element analysis is that, in the field, many natural exposures of cross-bedded facies cannot be directly related to deposits of macroforms. This may be because fields of ripples and dunes are genuinely genetically unrelated to their underlying surfaces, but often it may simply be because the vagaries of outcrop exposure prohibit an accurate understanding of the relationship between inclined foresets and their underlying surface.

In order to mitigate against any inherent uncertainty involved in the study of natural rock outcrops, in this study we differentiate between those architectural elements that we can classify definitively, and those which can only be identified with a degree of interpretation. To avoid conflation of observation and interpretation, if an accretion macroform was interpreted only and not directly measured, it was given the prefix 'i' (e.g., iDA, iLA) (Fig. 9). This prefix was also assigned to 'sandy-bedforms', which are here distinguished into two categories: (1) Those unambiguously unrelated to their underlying surface (SB); (2) Those which may or may not be genetically related, but where exposure prohibits an understanding of the relationship between inclined foresets and the underlying surface (iSB).

Within the Series Rouge, the vast majority of elements in depositional-strike successions, and the majority in depositional-dip successions were iSB. (Fig. 9).

4.2. Sheet-braided architecture of the Fréhel Formation

Sedimentary bodies in the Fréhel Formation either occur as *simple sheets* (Gibling, 2006), with aspect ratios regularly exceeding 75:1 (determining precise ratios is usually constrained by exposure), mostly recording in-channel dune migration, or as more *complex bar-forms*, representing both the migration

of accretion macroforms and in-channel dunes. The majority of *simple sheets* consist of 1 – 3 stacked sets of trough cross-stratification, with planar and laterally extensive set, co-set and sand-body bounding surfaces. *Complex bar-forms* are differentiated from simple-sheets by the presence of low-angle, inclined surfaces representing the incremental growth of individual bars. These accretion macroforms comprise different elements: whilst DA macroforms are by far the most abundant (Fig. 8C, Fig. 10A, Fig. 11C; Fig. 13), LA, DLA and UA macroforms also occur (Fig. 10, Fig. 11; Fig. 13). Co-set and set boundaries are typically inclined at greater angles than underlying incremental surfaces, and the lateral extent of individual surfaces is far less than in simple sheet-sandstones.

4.2.1. Stacked bar-forms at Pointe aux Chèvres

Stacked bar-forms crop out in coastal sections orientated parallel to depositional dip at Pointe aux Chèvres (Fig. 10). Fig. 10A shows accretion macroforms within 20 successive bar-forms.

Low-sinuosity accretion macroforms (DA, DLA) dominate this succession. Lateral-accretion surfaces (non-heterolithic) are apparent but uncommon. Some bar-forms display significant morphodynamic variation. For example, Figure 11A displays a preserved bar-form within which the mode of bedform migration can be seen to transition from net DLA (inclined cosets 30 - 60° from the underlying surface) to net DA (inclined cosets 0 - 30° from the underlying surface) over a distance of 15 m.

Depositional-strike exposures were also studied at Pointe aux Chèvre. These most commonly display sheet-braided architecture (aspect ratios >20: 1 (Cotter, 1978)), with thin, tabular sand-bodies extending laterally for at least 55 m. Channel-margins are notably rare (2 occurrences), but where present they exhibit < 1 m in erosional relief and are gently-dipping. Subordinate discontinuous bedding is apparent (Fig. 12), typically characterised by planar cross-stratification which diminishes in thickness towards sand-body margins. In one instance, discontinuous bedding is succeeded by a thin (<10 cm) red mudstone (possible bar-top hollow fill) (Fig. 12C). In thin section, this mud bore carbonaceous material and abundant detrital minerals (see Section 3; Fig. 12D).

4.2.2. Oblique to depositional-strike architecture at Sables d'Or Quarry

Quarry faces at Sables d'Or provide intermittent depositional-dip and depositional-strike exposure of both simple sheets and complex bar-forms, extending 1.3 km in total and >125 m continuously (Fig. 1). Sand-bodies are 1 – 3.5 m thick and commonly exceed exposure width; suggesting deposition as thin, narrow-broad sheets (*sensu* Gibling, 2006). No fine grained horizons were observed, but mud clasts are common.

Typical sand-body architecture is presented in Figure 13. Vertical cliff exposures were inaccessible in their upper levels; palaeocurrents were not estimated in these levels as they could not be directly measured.

Trough cross-stratification is near-ubiquitous, with cross-set thickness displaying no upwards decrease within individual bodies. No facies transition occurs across major surfaces, even on inclined surfaces representing bar-form growth. Major erosional bounding surfaces are dominantly planar. Reactivation surfaces bounding co-sets vary significantly in their lateral extent. In simple sheets, these surfaces are predominantly planar, and regularly extend laterally for over 60 m. Within bar-forms, gently dipping accretion surfaces rarely exceed 30 m before terminating against major erosional surfaces (Fig. 13). Gently inclined erosional scours also dissect individual sand-bodies, possibly representing fluctuating stages and bedform alignment within the overall system (e.g., Fahnestock, 1965; Cant and Walker, 1978; Miall, 2010).

Sandy-bedforms are the dominant element in depositional-strike/oblique exposures. Clear DA and DLA macroforms are discernible in places, but are inevitably less prominent than in depositional-strike successions. Inclined surfaces representing possible sandy lateral accretion (iLA) are present but have minimal contribution to the overall architecture (Fig. 13). Preserved channel margins are rare (4 occurrences) (Fig. 13). Maximum dip of channel-margins varies from 5 - 18°

4.2.3. Depositional-strike architecture at Îlot Saint-Michel

Figure 14 shows the interpreted architectural elements in a section from near the top of the formation at Îlot Saint-Michel. The section is orthogonal to slightly oblique to palaeoflow and shows numerous

448 low angle inclined surfaces here interpreted as iLA and iDLA elements. The figure also displays
449 discontinuous mudstone deposits.

450 **4.3. Interpretation of fluvial style**

451 The Fréhel Formation almost exclusively consists of stacked, sandstone sheets, typically 1 – 2 m
452 thick, with sedimentation dominated by in-channel dune migration, and with rarely observed channel
453 margins less than 0.5 m high. Stacked accretion macroforms (Fig. 11C) demonstrate that not all sand-
454 bodies were deposited in single episodes of flooding so flow may have been perennial (Bristow, 1987;
455 Best et al., 2003).

456 Mudrock is scarce in the Fréhel Formation (though becomes marginally more common up section).
457 This may relate to the poor preservation of bar top and floodplain facies: most sandbodies are
458 erosionally truncated, indicating only partial preservation of alluvium during river aggradation.
459 Alternatively the paucity of mudrock may reflect sediment bypass (due to highly variable discharge or
460 aeolian winnowing; Long, 1978; Dalrymple et al., 1985; Aspler and Chiarenzelli, 1997; Went, 2005)
461 or a lack of mud in the system (i.e., inherently low mud production due to the absence of vegetation-
462 mediated weathering; Davies & Gibling, 2010). The rare discontinuous mud lenses that are present
463 are interpreted to have been deposited in slackwater parts of the channel belt.

464 Bar-form orientations indicate that there was an overall low-sinuosity to the sand-dominated fluvial
465 system, with the majority of identified accretion macroforms only migrating 0 - 30° relative to
466 underlying, down-flow dipping surfaces. The near ubiquity of trough cross-stratification throughout
467 the sequence can be seen to be the result of normal in-channel sedimentation dominated by migrating
468 sinuous-crested dunes. Rare sandy lateral accretion surfaces likely reflect lateral accretion on
469 longitudinal bars within this low sinuosity system (Bristow, 1987).

470 The predominant sedimentary style of the Fréhel Formation is thus one of sheet-braided architecture
471 with very low mud content, likely reflecting sedimentation from a large, low-sinuosity, perennial (but
472 possibly seasonally-variable) braided river. Any larger-scale morphological variability, which is only
473 ever apparent in exceptionally extensive exposures of pre-vegetation alluvium (e.g., Ielpi and

Rainbird, 2016), cannot be assessed here due to Fréhel Formation exposure constraints. However, the sedimentary characteristics of the formation are consistent with typical pre-vegetation sandy alluvial successions, which typically present sheet-braided *architecture* (*sensu* Cotter, 1978) at normal outcrop scale (e.g., Long, 1978, 2006; Fedo and Cooper, 1990; Rainbird, 1992; McCormick and Grotzinger, 1993; Nicholson, 1993; MacNaughton et al., 1997; Eriksson et al., 1998; Köykkä, 2011; Marconato et al., 2014; Ielpi and Rainbird, 2015).

5. Reasons to doubt matgrounds as stabilizing agents

The meso-scale sheet-braided architecture of the Fréhel Formation (Section 4) demonstrates that there is no evidence suggesting that matgrounds (Section 3) offered any level of landscape stability to the Series Rouge fluvial systems that could be compared to that provided by land plants in Silurian and younger counterparts. This is contrary to studies that have hypothesised that microbial mats might have fulfilled a similar role to land plants, as geomorphic stabilizers, on pre-vegetation Earth (e.g., Bose et al., 2012; Petrov, 2014, 2015; Santos & Owen, 2016; Ielpi, 2016). However, this is perhaps unsurprising as, in order for biostabilization to significantly affect fluvial deposits, it is vital that any biological cohesion exceeds physical erosive forces. Four lines of evidence suggest that microbial mats do not and could not have provided such requisite levels of cohesion, and are discussed in the following sections.

5.1. Matgrounds are surficial features

One key difference between matgrounds and higher land plants is that the latter have deep substrate anchorage, accentuated by palimpsesting of multiple generations of roots. The increased cohesion associated with such underground roots has been demonstrated to provide reinforcement of bank sediments (e.g., Smith, 1976; Bridge, 1993), increasing the critical shear stress of river banks and limiting undercutting. In a classic study, Smith (1976) demonstrated that, within the Alexandra Valley (Canada), grass roots on the floodplain margins of river channels accumulated down to depths of 7.6 metres; far in excess of the depth required to reinforce banks against caving (in this instance, 3.5 metres – the depth of the adjacent channel). Conversely, modern microbial mats attain maximum

thicknesses of several centimetres and only persist near the substrate surface (de Beer and Kühl, 2001) due to their rapid decomposition following burial by even thin event layers of sediment (e.g. Black, 1933; Krumbein and Stuart, 1983; Chafetz and Buczynski, 1992; Konhauser, 2007).

Considering that the limited root penetration of the earliest embryophytes (Edwards et al., 2015) had a limited effect on alluvial architecture, and that bank stabilization by roots did not develop until deeper rooting near the Siluro-Devonian boundary (e.g., Gensel et al., 2001; Hillier et al., 2008; Davies & Gibling, 2010; Kennedy et al., 2012), it is unsurprising that even less-penetrative surficial mats left no evidence for having any effect on bank stability. Microbial mats can offer no protection against the undercutting of substrates on which they rest, yet bank undercutting is the primary erosive mechanism of lateral fluvial channel migration.

A further difference between microbial mats and land plants is the latter frequently alter surface microtopograhy which in turn reduces flow velocity (Bouma et al., 2013; Moor et al., 2017).

5.2. Matground properties change when emergent

A further difference between microbial mats and land plants is that the latter have the capacity to develop structure above the water-table and do not necessarily undergo changes to their physical properties (as mechanical components of the fluvial system) whether they are submerged, wet, or dry. In contrast, matgrounds exist in an elastic state when they are respiring, but only respire when they are submerged in water. When they dry out and stop respiring, they behave in a brittle fashion and may easily become detached from a substrate through desiccation, shrinkage and curling. The bulk of studies that have looked at the sedimentological influences of microbiota are usually only concerned with mats in their elastic state (e.g., Gerdes, 2007; Hagadorn and McDowell, 2012; Vignaga et al., 2013). Even when substrates are wet, matgrounds may still detach (1) if the physical forces acting on them exceed their biological cohesiveness (Moulin et al., 2008; Graba et al., 2010, 2013, 2014); or (2) by autogenic buoyancy-mediated detachment processes (Boulêtreau et al., 2006; Mendoza-Lera et al., 2016).

As river channel migration occurs primarily through undercutting of *emergent* substrates, it should be expected that those mats on raised banks adjacent to active channels would usually comprise dried, surficial microbial mats that would provide negligible reinforcement against bank erosion (although biological soil crusts may be an exception).

5.3. There are no modern analogues of matground-stabilized rivers

To our knowledge, there are no published studies of modern rivers that suggest that microbial mat or biological soil crust communities can stabilize river banks. Modern rivers that exist in the complete absence of any form of vegetation are rare or non-existent at the present day (Davies et al., 2011). However, partial analogues may be seen in rivers that exist in climatic extremes, and glaciofluvial braidplains have been considered to have some resemblance to pre-vegetation rivers (Cotter, 1982; Davies et al., 2011; Ielpi and Rainbird, 2016). Figure 15 illustrates examples of microbial communities living in and adjacent to such a braidplain of the Mimer River in Spitsbergen. Biofilms exist in slackwater or sluggish lotic conduits of water and chute channels on braid bars, but are absent in the main trunk channels. Isolated examples of the cyanobacteria *Rivularia* are seen co-exisiting with mosses on top of subaerial bar forms. Neither of these microbiota are well-anchored to the substrate and would become readily detached and removed when the river entered spate during spring melt. The margins of the braidplain (and some of the more elevated bar tops) have been colonized by communities of biological soil crusts, as well as shallow rooted tracheophytes. However, these can be seen to be being actively unroofed by undercutting from flowing water in adjacent trunk channels, and the integrity of unroofed clasts of soil crust is largely maintained by plant roots. These modern observations attest to the limited resistance to fluvial erosion offered by microbiota.

5.4. There is no physical evidence in the rock record for matground stabilized rivers

There are relatively few records of observed microbial matground fabrics within pre-vegetation alluvial strata (e.g., Sheldon, 2012; Beraldi-Campesi et al., 2014; Wilmeth et al., 2014); although some studies have speculated on a hypothesised alluvial microbiota (e.g., Santos and Owen, 2016). The modern examples of microbiota from the sparsely vegetated Mimer River (Fig. 15) provide a

potentially analogous explanation for this paucity of matground evidence in ancient alluvium. If their pre-vegetation counterparts occupied similar reaches of ancient braidplains, it should be expected that they would have very limited preservation potential in the rock record: lacking the capacity to resist physical reworking, they essentially occupy erosional, rather than depositional, subenvironments of the fluvial system. Their occurrence in the rock record is thus limited to fortuitous instances where components of such subenvironments have only undergone partial erosion (e.g., the rare mud horizons or intraformational clasts of the Fréhel Formation).

The limitations of microbial mats as pre-vegetation stabilizers of alluvial landscapes are further revealed by the global stratigraphic record of microbially-induced sedimentary structures. In a table demonstrating previously-published reports of MISS, and the facies from which they were recorded, Davies et al. (2016, their Table 1) listed only 5 instances of pre-vegetation fluvial MISS (8.2% of the total Precambrian to mid Silurian records across all sedimentary environments), compared to 11 instances of post-vegetation MISS (31.4% of the total late Silurian to Cretaceous records). This suggests that, while MISS were present in Earth's fluvial environments since at least the Proterozoic, they were far more commonly preserved after the evolution of land plants. That is, once the more muddy and quiescent fluvial subenvironments most commonly colonized by microbial mats (floodplains, etc.) began to become deeply stabilized by roots, less prone to wholesale reworking during deposition, and more readily preserved in the rock record. This observation provides further circumstantial evidence that the stabilization, and preservation potential, of certain fluvial facies afforded by terrestrial vegetation was several orders of magnitude greater than that afforded by microbial mats alone.

6. Conclusion

The Series Rouge of northwest France contains a wealth of individual circumstantial lines of evidence for the presence of microbial mats which, combined, suggest that the fluvial systems active during deposition operated within a 'microbial landscape'. Despite this, there is no evidence that microbial mats increased the stability of any components of the fluvial system. The fluvial deposits are

578 characterised by repetitively stacked beds of trough cross-stratified sandstone representing deposition
579 from migrating sinuous crested dunes in low sinuosity channels and on predominantly downcurrent-
580 dipping compound bars. Frequent channel-switching led to selective preservation of deep channel-bar
581 deposits such that the preserved sedimentary architecture is sheet-braided at outcrop scale; the typical
582 stratigraphic record of many other pre-vegetation fluvial systems.

583 Through a critical understanding of the ways in which microbial mats may affect sedimentation,
584 coupled with partial modern analogues and reference to the global stratigraphic record of alluvial
585 microbially induced sedimentary structures, it is shown that microbial mats alone were very weak
586 agents of geomorphic stabilization. In the pre-vegetation world, they were several orders of
587 magnitude less effective at buffering against erosion when compared to the land plants that began to
588 share their nonmarine habitats from the Palaeozoic onwards (Figure 16). The influence of microbial
589 mats on the sedimentary characteristics of pre-vegetation alluvium is thus shown to have been
590 negligible. With such ineffective biotic feedback to river functioning, pre-vegetation fluvial systems
591 were perpetually trapped in the simplest geomorphic phase of fluvial biogeomorphic succession
592 (*sensu* Corenblit et al., 2014). As a result, the stratigraphic sedimentary record is biased in only
593 preserving a record of the dominant purely physical processes in such systems.

594 Despite this, microbiota did apparently leave much smaller scale clues to their presence and activity
595 within pre-vegetation systems. In the Series Rouge, these include a suite of potential microbial
596 sedimentary surface textures, distinct "pseudofossils" such as *Aristophycus* and *Arumberia*, and
597 petrographic indicators, such as biotite accumulations and associated carbonaceous laminae. This
598 indicates that some of the oldest communities of life on land were able to bestow an influence on the
599 long-term rock record, even though they lacked an ecosystem engineering capacity to geomorphically
600 sculpt the landscapes that they once inhabited.

601 **Acknowledgements**

602 Supported by Shell International Exploration and Production B.V under Research Framework
603 agreement PT38181. We would also like to thank Martin Gibling and Sanjeev Gupta for their

constructive comments on the first draft of this manuscript. Reviewers Darrel Long and Chris Fedo and editor Randall Parish are gratefully acknowledged for their constructive comments on the paper.

References

Algeo, T.J., Scheckler, S.E., 1998. Terrestrial–marine teleconnections in the Devonian: links between the evolution of land plants, weathering processes, and marine anoxic events. Philosophical Transactions of the Royal Society of London B 353, 113–130.

Allen, J.R.L., 1982. Sedimentary Structures: Their Character and Physical Basis. Elsevier, Amsterdam

Allen, J.R.L., 1983. Studies in fluviatile sedimentation: bars, bar-complexes and sandstone sheets (low-sinuosity braided streams) in the Brownstones (L. Devonian), Welsh Borders. Sedimentary Geology 33, 237-293.

Aspler, L.B., Chiarenzelli, J.R., 1997. Initiation of 2.45–2.1 Ga intracratonic basin sedimentation of the Hurwitz Group, Keewatin Hinterland, Northwest Territories, Canada. Precambrian Research 81, 265–297.

Astin, T.R., Rogers, D.A., 1991. "Subaqueous shrinkage cracks" in the Devonian of Scotland reinterpreted. J. Sediment. Res. 61, 850–859.

Auvray, B., 1979. Genese et evolution de la croftte continentale dans Ie Nord du Massif armoricain. These, Rennes University.

Auvray, B., Macé, J., Vidal, P., Vander Voo, R., 1980. Rb-Sr dating of the Plouézec volcanics, N Brittany: implications for the age of red beds ('Series rouges') in the northern Armorican Massif. Journal of the Geological Society 137, 207-210.

Beraldi-Campesi, H., Farmer, J. D., Garcia-Pichel, F., 2014. Modern terrestrial sedimentary biostructures and their fossil analogs in Mesoproterozoic subaerial deposits. Palaios 29, 45-54.

633 Best, J.L., Ashworth, P.J., Bristow, C.S., Roden, J., 2003. Three-dimensional sedimentary architecture of a
634 large, mid-channel sand braid bar, Jamuna River, Bangladesh. Journal of Sedimentary Research 73, 516-530.
635
636 Black, M., 1933. The algal sediments of Andros Island, Bahamas: Philosophical Transactions of the Royal
637 Society of London, Series B 222, 165-192.
638
639 Bland, B.H., 1984. Arumberia Glaessner & Walter, a review of its potential for correlation in the region of the
640 Precambrian–Cambrian boundary. Geological Magazine 121, 625-633.
641
642 Boulêtreau, S., Garabetian, F., Sauvage, S., Sanchez-Perez, J.M., 2006. Assessing the importance of a self-
643 generated detachment process in river biofilm models. Freshwater Biol. 51, 901–912,
644
645 Bosak, T., Bush, J.W.M., Flynn, M.R., Liang, B., Ono, S., Petroff, A.P., Sim, M.S., 2010. Formation and
646 stability of oxygen-rich bubbles that shape photosynthetic mats. Geobiology 8, 45–55
647
648 Bose, P.K., Eriksson, P.G., Sarkar, S., Wright, D.T., Samanta, P., Mukhopadhyay, S., Mandal, S., Banerjee, S.,
649 and Altermann, W., 2012. Sedimentation patterns during the Precambrian: a unique record?. Marine and
650 Petroleum Geology 33, 34-68.
651
652 Bouma, T.J., Temmerman, S., van Duren, L.A., Martini, E., Vandenbruwaene, W., Callaghan, D.P., Balke, T.,
653 Biermans, G., Klaassen, P.C., van Steeg, P. and Dekker, F., 2013. Organism traits determine the strength of
654 scale-dependent bio-geomorphic feedbacks: A flume study on three intertidal plant species. *Geomorphology*
655 *180*, pp.57-65.
656
657 Brasier, M.D., 1979. The Cambrian radiation event, p. 103 – 159. In: The Origin of the Major Invertebrate
658 Groups (Ed. House, M.R.), Academic Press London Systematics Association Sp. Vol. 12.
659
660 Bridge, J.S., 1993. The interaction between channel geometry, water flow, sediment transport and deposition in
661 braided rivers. Geological Society, London, Special Publications 75, 13-71.
662

Bristow, C.S., 1987. Brahmaputra River: channel migration and deposition.

Cant, D.J., & Walker, R.G., 1978. Fluvial processes and facies sequences in the sandy braided South Saskatchewan River, Canada. Sedimentology 25, 625-648.

Chafetz, H. S., Buczynski, C., 1992. Bacterially induced lithification of microbial mats. Palaios, 277-293.

Corenblit, D., Steiger, J., González, E., Gurnell, A.M., Charrier, G., Darrozes, J., Dousseau, J., Julien, F., Lambs, L., Larrue, S. and Roussel, E., 2014. The biogeomorphological life cycle of poplars during the fluvial biogeomorphological succession: a special focus on Populus nigra L. Earth Surface Processes and Landforms 39, 546-563.

Cotter, E., 1982, Tuscarora Formation of Pennsylvania. Guidebook, SEPM, May 8 and 9, 1982/Eastern Section field trip. Bucknell University, Lewisburg, Pennsylvania, 105

Cotter, E., 1978. The evolution of fluvial style, with special reference to the central Appalachian Paleozoic. In: Miall, A.D. (Ed.), Fluvial Sedimentology: Canadian Society of Petroleum Geologists Memoir, vol. 5, pp. 361–383.

Dabard, M.P., Guillocheau, F., Loi, A., Paris, F., Balèvre, M., 2009. Evolution de la plate-forme paléozoïque centre-armoricaine del'Ordovicien au Dévonien. 12ème Congrès Français de Sédimentologie, Rennes, 2009. Livret d'excursions. Presqu'Ile de Crozon. Publication ASF 65, 55-102.

Dabard, M.P., Loi, A., Paris, F., 2007. Relationship between phosphogenesis and sequence architecture: sequence stratigraphy and biostratigraphy in the Middle Ordovician of the Armorican Massif (W France). Palaeogeography, Palaeoclimatology, Palaeoecology 248, 339–356.

Dalrymple, R.W., Narbonne, G.M., Smith, L., 1985. Eolian action and the distribution of Cambrian shales in North America. Geology 13, 607–610.

Davies, N.S., Gibling, M.R., 2010. Cambrian to Devonian evolution of alluvial systems: the sedimentological impact of the earliest land plants. Earth-Science Reviews 98, 171-200.

692

693 Davies, N.S., Gibling, M.R., Rygel, M.C., 2011. Alluvial facies evolution during the Palaeozoic greening of the
694 continents: case studies, conceptual models and modern analogues. Sedimentology 58, 220-258.
695
696 Davies, N.S., Liu, A.G., Gibling, M.R. and Miller, R.F., 2016. Resolving MISS conceptions and
697 misconceptions: A geological approach to sedimentary surface textures generated by microbial and abiotic
698 processes. Earth-Science Reviews 154, 210-246.
699
700 Davies, N.S., Shillito, A.P., McMahon, W.J., 2017. Short-term evolution of primary sedimentary surface
701 textures (microbial, ichnological) on a dry stream bed: modern observations and ancient implications. Palaios, in
702 press. DOI: http://dx.doi.org/10.2110/palo.2016.064
703
704 De Beer, D., Kühl, M., 2001. Interfacial microbial mats and biofilms. In: Boudreau, B.P., Jørgensen, B.B.,
705 (eds.), The Benthic Boundary Layer. Oxford University Press, New York, 2001.
706
707 De Boer, P., 1979. Convolute lamination of modern sands in the estuary of the Oosterschelde, the Netherlands,
708 formed as a result of trapped air. Sedimentology 26, 283–294.
709
710 Deb, S.P., Schieber, J., Chaudhuri, A.K., 2007. Microbial mat features in mudstones of the Mesoproterozoic
711 Somanpalli Group, Pranhita-Godavari Basin, India.
712
713 D'lemos, R.S., Miller, B.V., Samson, S.D., 2001. Precise U–Pb zircon ages from Alderney, Channel Islands:
714 growing evidence for discrete Neoproterozoic magmatic episodes in northern Cadomia. Geological magazine
715 138, 719-726.
716
717 D'Lemos, R.S., Strachan, R.A., Topley, C.G., 1990. The Cadomian orogeny in the North Armorican Massif: a
718 brief review. Geological Society, London, Special Publications 51, 3-12.
719
720 Doré, F., 1972. La transgression majeure du Paleozoique inferieur dans Ie Nord-Est du Massif armoricain. Bull
721 Soc Geol Fr, 7145, 801-814

Doré, F., 1994. Cambrian of the Armorican massif. In *Pre-Mesozoic Geology in France and Related Areas* (pp. 136-141). Springer Berlin Heidelberg.

Dornbos, S.Q., Noffke, N. and Hagadorn, J.W., 2007. 4 (d). Mat-decay features. Atlas of microbial mats features preserved within the siliciclastic rock record. Atlases in Geosciences 2, 106-110.

Doyle, L.J., Carder, K.L., Steward, R.G., 1983. The hydraulic equivalence of mica. Journal of Sedimentary Research 53, 643-648.

Driese, S.G., Jirsa, M.A., Ren, M., Brantley, S.L., Sheldon, N.D., Parker, D., Schmitz, M., 2011. Neoarchean paleoweathering of tonalite and metabasalt: Implications for reconstructions of 2.69 Ga early terrestrial ecosystems and paleoatmospheric chemistry. Precambrian Research 189, 1-17.

Edwards, D., Cherns, L. and Raven, J.A., 2015. Could land-based early photosynthesizing ecosystems have bioengineered the planet in mid-Palaeozoic times?. Palaeontology 58, 803-837.

Els, B.G., Van den Berg, W.A., & Mayer, J.J., 1995. The Black Reef Quartzite Formation in the western Transvaal: sedimentological and economic aspects, and significance for basin evolution. Mineralium Deposita 30, 112-123.

Eriksson, P.G., Condie, K.C., Tirsgaard, H., Mueller, W.U., Altermann, W., Miall, A.D., Aspler, L.B., Catuneanu, O., Chiarenzelli, J.R., 1998. Precambrian clastic sedimentation systems. Sedimentary Geology, 120 5-53.

Eriksson, P.G., Wright, D.T., Bumby, A.J., Catuneanu, O., Mostert, P., 2009. Possible evidence for episodic epeiric marine and fluvial sedimentation (and implications for palaeoclimatic conditions), c. 2.3–1.8 Ga, Kaapvaal craton, South Africa. Palaeogeography, Palaeoclimatology, Palaeoecology 273, 153-173.

751 Fahnestock, R.K., 1965. Stratification, bed forms, and flow phenomena (with an example from the Rio Grande):
752 in GV Middleton, ed. Soc. Econ. Paleontologists and Mineralogists, Spec. Pub 12, 84-115.
753
754 Fedo, C. M., Cooper, J. D., 1990. Braided fluvial to marine transition: the basal Lower Cambrian Wood Canyon
755 Formation, southern Marble Mountains, Mojave Desert, California. Journal of Sedimentary Research 60.
756
757 Fordham, A.W., 1990. Weathering of biotite into dioctahedral clay minerals. Clay Minerals 25, 51-63.
758
759 Friend, P.L., Lucas, C.H., Holligan, P.M., Collins, M.B., 2008. Microalgal mediation of ripple mobility.
760 Geobiology 6, 70–82.
761
762 Gehling, J.G., 1999. Microbial mats in terminal Proterozoic siliciclastics; Ediacaran death masks. Palaios 14,
763 40-57.
764
765 Gehling, J.G., Droser, M.L., 2009. Textured organic surfaces associated with the Ediacara biota in South
766 Australia. Earth-Science Reviews 96, 196-206.
767
768 Gensel, P.G., Kotyk, M.E., Basinger, J.F., 2001. Morphology of above- and below-ground structures in Early
769 Devonian (Pragian-Emsian) plants. In Gensel, P.G., Edwards, D., eds. Plants Invade the Land: Evolutionary and
770 Environmental Perspectives. Columbia University Press, New York, 83–102
771
772 Gerdes, G., 2007. Structures left by modern microbial mats in their host sediments. Atlas of microbial mat
773 features preserved within the clastic rock record. Elsevier, Amsterdam, 5-38.
774
775 Gerdes, G., Krumbein, W.E., 1987. Biolaminated Deposits. Lecture Notes in Earth Sciences 9, Springer, New
776 York, 183 pp.
777
778 Germs, G.J.B., 1983. Implications of a sedimentary facies and depositional environmental analysis of the Nama
779 Group in South West Africa (Namibia). Spec. Publ. Geol. Soc. Afr. 11, 89-114
780

781 Gibling, M.R., 2006. Width and thickness of fluvial channel bodies and valley fills in the geological record: a
782 literature compilation and classification. Journal of sedimentary Research 76, 731-770.
783
784 Gibling, M.R., Davies, N.S., Falcon-Lang, H.J., Bashforth, A.R., DiMichele, W.A., Rygel, M.C., Ielpi, A.,
785 2014. Palaeozoic co-evolution of rivers and vegetation: a synthesis of current knowledge. Proceedings of the
786 Geologists' Association 125, 524-533.
787
788 Glaessner, M.F., Walter, M.R., 1975. New Precambrian fossils from the Arumbera Sandstone, Northern
789 Territory, Australia. Alcheringa 1, 59-69.
790
791 Graba, M., Moulin, F.Y., Boulêtreau, S., Garabétian, F., Kettab, A., Eiff, O., Sánchez-Pérez, J.M., Sauvage, S.,
792 2010. Effect of near-bed turbulence on chronic detachment of epilithic biofilm: Experimental and modeling
793 approaches. Water Resources Research 46.
794
795 Graba, M., Sanchez–Perez, J.M., Moulin F.Y., Urrea, G., Sabater, S., Sauvage S., 2013. Interaction between
796 local hydrodynamics and algal community in epilithic biofilm. Water Research 47, 2153–2163.
797
798 Graba, M., Sauvage, S., Majdi, N., Mialet, B., Moulin, F. Y., Urrea, G., Sanchez-Pérez, J. M., 2014. Modelling
799 epilithic biofilms combining hydrodynamics, invertebrate grazing and algal traits. Freshwater biology 59, 1213-
800 1228.
801
802 Hagadorn, J.W., Mcdowell, C., 2012. Microbial influence on erosion, grain transport and bedform genesis in
803 sandy substrates under unidirectional flow. Sedimentology 59, 795-808.
804
805 Hagstrum, J.T., Van der Voo, R., Auvray, B., Bonhommet, N., 1980. Eocambrian—Cambrian palaeomagnetism
806 of the Armorican Massif, France. Geophysical Journal International 61, 489-517.
807
808 Harazim, D., Callow, R. H., Mcilroy, D., 2013. Microbial mats implicated in the generation of intrastratal
809 shrinkage ('synaeresis') cracks. Sedimentology 60, 1621-1638.
810

Harrison, P.A., 1979. The structure and sedimentology of the Sinclair Group in the Awasib Mountains, DiamondArea No. 2, South West Africa/Namibia. B.Sc. (Hons.) thesis (unpubl.), Rhodes University, Grahamstown, 69 pp.

Hill, C., Corcoran, P.L., Aranha, R., Longstaffe, F. J., 2016. Microbially induced sedimentary structures in the Paleoproterozoic, upper Huronian Supergroup, Canada. Precambrian Research.

Hillier, R.D., Edwards, D., Morrissey, L.B., 2008. Sedimentological evidence for rooting structures in the Early Devonian Anglo-Welsh Basin (UK), with speculation on their producers. Palaeogeography Palaeoclimatology Palaeoecology 270, 366–380.

Horodyski, R.J., Bloeser, B., Von der Haar, S., 1977. Laminated algal mats from a coastal lagoon, Laguna Mormona, Baja California, Mexico. J. Sediment. Petrol. 47, 680–696.

Horodyski, R.J., Knauth, L.P., 1994. Life on land in the Precambrian. Science-AAAS-Weekly Paper Edition-including Guide to Scientific Information 263, 494-498.

Ielpi, A. 2016. Lateral accretion of modern unvegetated rivers: remotely sensed fluvial–aeolian morphodynamics and perspectives on the Precambrian rock record.

Ielpi, A., Ghinassi, M., 2015. Planview style and palaeodrainage of Torridonian channel belts: Applecross Formation, Stoer Peninsula, Scotland. Sediment. Geol. 325, 1-16.

Ielpi, A., Ghinassi, M., 2016. A sedimentary model for early Palaeozoic fluvial fans, Alderney Sandstone Formation (Channel Islands, UK). Sedimentary Geology 342, 31-46.

Ielpi, A., Rainbird, R.H., 2015. Architecture and morphodynamics of a 1.6 Ga fluvial sandstone: Ellice Formation of Elu Basin, Arctic Canada. Sedimentology 62, 1950-1977.

Ielpi, A., Rainbird, R.H., 2016. Reappraisal of Precambrian sheet-braided rivers: Evidence for 1.9 Ga deep-channelled drainage. Sedimentology.

Kemp, J., 1996. The Kuara Formation (northern Arabian Shield); definition and interpretation: a probable fault-trough sedimentary succession. Journal of African Earth Sciences 22, 507-523.

Kennedy, K.L., Gensel, P.G., Gibling, M.R., 2012. Paleoenvironmental inferences from the classic Lower Devonian plant-bearing locality of the Campbellton Formation, New Brunswick, Canada. Palaios 27, 424–438.

Knaust, D., Hauschke, N., 2004. Trace fossils versus pseudofossils in Lower Triassic playa deposits, Germany. Palaeogeography, Palaeoclimatology, Palaeoecology 215, 87-97.

Kolesnikov, A.V., Grazhdankin, D.V., Maslov, A.V., 2012. Arumberia-type structures in the Upper Vendian of the Urals. In Doklady Earth Sciences (Vol. 447, No. 1, pp. 1233-1239). SP MAIK Nauka/Interperiodica.

Konhauser, K., 2007. Introduction to Geomicrobiology. Blackwell, Oxford (425 pp.).

Köykkä, J., 2011. The sedimentation and paleohydrology of the Mesoproterozoic stream deposits in a strike–slip basin (Svinsaga Formation), Telemark, southern Norway. Sedimentary Geology 236, 239-255.

Krumbein, WE, Cohen Y (1977) Primary production, mat formation and lithification: contribution of oxygenic and facultative an oxygenic cyanobacteria. In: Flugel E (ed) Fossil algae. Springer, Berlin Heidelberg New York, 37–56

Krumbein, W.E., Paterson, D.M., Stal, L., 1994. Biostabilization of Sediments. Bibliotheks und Informationsystem, Oldenburg, Germany, 526.

Krumbein, W.E., Swart, P.K., 1983. The microbial carbon cycle: in Krumbein, W.E., ed., Microbial Geochemistry: Blackwell Scientific Publishers, Oxford, 5-62.

870 Kumar, S., Ahmad, S., 2014. Microbially induced sedimentary structures (MISS) from the Ediacaran Jodhpur
871 Sandstone, Marwar Supergroup, western Rajasthan. Journal of Asian Earth Sciences 91, 352-361.
872
873 Long, D.G.F., 1978. Proterozoic stream deposits: some problems of recognition and interpretation of ancient
874 sandy fluvial systems. In: Miall, A.D. (Ed.), Fluvial Sedimentology: Canadian Society of Petroleum Geologists
875 Memoir, vol. 5, 313–341.
876
877 Long, D.G.F., 2006. Architecture of pre-vegetation sandy-braided perennial and ephemeral river deposits in the
878 Paleoproterozoic Athabasca Group, northern Saskatchewan, Canada as indicators of Precambrian fluvial style.
879 Sedimentary Geology 190, 71–95.
880
881 Long, D.G.F., 2011. Architecture and depositional style of fluvial systems before land plants: a comparison of
882 Precambrian, early Paleozoic and modern river deposits. From River to Rock Record: The Preservation of
883 Fluvial Sediments and their Subsequent Interpretation: SEPM, Special Publication 97, 37-61.
884
885 MacNaughton, R.B., Dalrymple, R.W., Narbonne, G.M., 1997. Early Cambrian braid-delta deposits, MacKenzie
886 Mountains, north-western Canada. Sedimentology 44, 587-609.
887
888 Marconato, A., de Almeida, R.P., Turra, B.B., dos Santos Fragoso-Cesar, A. R., 2014. Pre-vegetation fluvial
889 floodplains and channel-belts in the Late Neoproterozoic–Cambrian Santa Bárbara group (Southern Brazil).
890 Sedimentary Geology 300, 49-61.
891
892 Malarkey, J., Baas, J.H., Hope, J.A., Aspden, R.J., Parsons, D.R., Peakall, J., Paterson, D.M., Schindler, R.J.,
893 Ye, L., Lichtman, I.D., Bass, S.J., 2015. The pervasive role of biological cohesion in bedform development.
894 Nature communications 6.
895
896 McCormick, D.S., Grotzinger, J.P., 1993. Distinction of marine from alluvial facies in the Paleoproterozoic (1.9
897 Ga) Burnside Formation, Kilohigok Basin, N.W.T., Canada. Journal of Sedimentary Petrology 63, 398–416.
898

McIlroy, D., Walter, M.R., 1997. A reconsideration of the biogenicity of Arumberia banksi Glaessner & Walter. Alcheringa 21, 79-80.

Medaris Jr, L.G., Singer, B. S., Dott Jr, R.H., Naymark, A., Johnson, C.M., Schott, R.C., 2003. Late Paleoproterozoic climate, tectonics, and metamorphism in the southern Lake Superior region and Proto–North America: evidence from Baraboo interval quartzites. The Journal of geology 111, 243-257.

Mendoza-Lera, C., Federlein, L.L., Knie, M., Mutz, M., 2016. The algal lift: Buoyancy-mediated sediment transport. Water Resources Research.

Miall, A.D., 1985. Architectural-element analysis: a new method of facies analysis applied to fluvial deposits.

Miall, A.D., 1996. The Geology of Fluvial Deposits. Springer. New York , 582.

Miall, A.D., 2010. Architectural-element analysis: a new method of facies analysis applied to fluvial deposits. Recognition of fluvial depositional systems and their resource potential 1, 33.

Miller, B.V., Samson, S.D., D'Lemos, R.S., 2001. U–Pb geochronological constraints on the timing of plutonism, volcanism, and sedimentation, Jersey, Channel Islands, UK. Journal of the Geological Society 158, 243-251.

Moor, H., Rydin, H., Hylander, K., Nilsson, M. B., Lindborg, R., & Norberg, J., 2017. Towards a trait-based ecology of wetland vegetation. Journal of Ecology.

Moulin, F.Y., Peltier, Y., Bercovitz, Y., Eiff, O., Beer, A., Pen, C., Boulêtreau, S., Garabétian, F., Sellali, M., Sànchez-Pérez, J., Sauvage, S., 2008. Experimental study of the interaction between a turbulent flow and a river biofilm growing on macrorugosities. Freshwater Biology 36, 249-263.

927 Nicholson, P.G., 1993. A basin reappraisal of the Proterozoic Torridon Group, northwest Scotland. In: Tectonic
928 Controls and Signatures in Sedimentary Successions (Eds L.E. Frostick and R.J. Steel), Spec. Pub. Int. Ass.
929 Sediment. 20, 183-202.
930
931 Noffke, N., 2010. Geobiology: Microbial Mats in Sandy Deposits from the ArcheanEra to Today. Springer-
932 Verlag, Berlin, pp. 194.
933
934 Noffke, N., Gerdes, G., Klenke, T., Krumbein, W. E. 2001. Microbially Induced Sedimentary Structures-A New
935 Category within the Classification of Primary Sedimentary Structures: PERSPECTIVES. Journal of
936 Sedimentary Research 71, 649-656.
937
938 Noffke, N., Gerdes, G., Klenke, T., Krumbein,W.E., 1996. Microbially induced sedimentary structures-
939 examples from modern sediments of siliciclastic tidal flats. Zentralbl. Geol. Palaeontol. Teil 1, 307–316 (Heft,
940 1/2).
941
942 Osgood, R.G., 1970. Trace fossils of the Cincinnati area. Paleontological Research Institution.
943
944 Paris, F., Robardet, M., Dabard, M.P., Feist, R., Ghienne, J.F., Guillocheau, F., Le Hérissé, A., Loi, A., Mélou,
945 M., Servais, T., Shergold, J., Vidal, M., Vizcaïno, D., 1999. Ordovician sedimentary rocks of France. Acta
946 Universitatis Carolinae, Geologica 43, 85–88.
947
948 Parizot, M., Eriksson, P.G., Aifa, T., Sarkar, S., Banerjee, S., Catuneanu, O., Altermann, W., Bumby, A.J.,
949 Bordy, E.M., van Rooy, J.L., Boshoff, A.J., 2005. Suspected microbial mat-related crack-like sedimentary
950 structures in the Palaeoproterozoic Magaliesberg Formation sandstones, South Africa. Precambrian Research
951 138, 274-96.
952
953 Pasteels, P., Doré, F., 1982. Age of the Vire-Carolles granite. In: Odin G (ed) Numerical dating in stratigraphy.
954 John Wiley, New York, 784-790
955

Petrov, P.Y., 2014. The Mukun basin: Settings, paleoenvironmental parameters, and factors controlling the early mesoproterozoic terrestrial sedimentation (Lower Riphean section of the Anabar uplift, Siberia). Lithology and Mineral Resources 49, 55-80.

Petrov, P.Y., 2015. Microbial factor in the formation of sedimentary continental systems of the Proterozoic (Mukun Basin, Lower Riphean of the Anabar Uplift of Siberia). Paleontological Journal 49, 530-545.

Pillola, G. I., 1993. The Lower Cambrian trilobite Bigotina and allied genera. Palaeontology 36, 855-855.

Pratt, B.R., 1998. Syneresis cracks: subaqueous shrinkage in argillaceous sediments caused by earthquake-induced dewatering. Sediment. Geol. 117, 1–10.

Prave, A. R., 2002. Life on land in the Proterozoic: Evidence from the Torridonian rocks of northwest Scotland. Geology 30, 811-814.

Rainbird, R.H., 1992. Anatomy of a large-scale braid-plain quartzarenite from the Neoproterozoic Shaler Group, Victoria Island, Northwest Territories, Canada. Canadian Journal of Earth Sciences 29, 2537-2550.

Rasmussen, B., Blake, T.S., Fletcher, I.R., Kilburn, M.R., 2009. Evidence for microbial life in synsedimentary cavities from 2.75 Ga terrestrial environments. Geology 37, 423-426.

Renouf, L.T., 1974. The Proterozoic and Palaeozoic development of the Armorican and Cornubian provinces. Proceedings of the Ussher Society 3, 6-43.

Runnegar, B.N., Fedonkin, M.A., 1992. Proterozoic Metazoan Body Fossils. In: Schopf, J.W., Klein, C. (Eds.), The Proterozoic Biosphere: A Multidisciplinary Study. Cambridge University Press, pp. 369–388.

Samanta, P., Mukhopadhyay, S., Mondal, A., Sarkar, S., 2011. Microbial mat structures in profile: the Neoproterozoic Sonia sandstone, Rajasthan, India. Journal of Asian Earth Sciences, 40, 542-549.

Santos, M.G., Almeida, R.P., Godinho, L.P., Marconato, A., Mountney, N.P., 2014. Distinct styles of fluvial deposition in a Cambrian rift basin. Sedimentology 61, 881-914.

Santos, M.G., Owen, G., 2016. Heterolithic meandering-channel deposits from the Neoproterozoic of NW Scotland: Implications for palaeogeographic reconstructions of Precambrian sedimentary environments. Precambrian Research 272, 226-243.

Sarkar, S., Banerjee, S., Eriksson, P.G., & Catuneanu, O., 2005. Microbial mat control on siliciclastic Precambrian sequence stratigraphic architecture: examples from India. Sedimentary Geology 176, 195-209.

Schieber, J., 1998. Possible indicators of microbial mat deposit in shale and sandstones: example from the Mid-Proterozoic Belt Supergroup, Montana, USA. Sed. Geol. 120, 105–124.

Schieber, J., 1999. Microbial mats in terrigenous clastics; the challenge of identification in the rock record. Palaios 14, 3-12.

Schieber, J., 2004. Microbial mats in the siliciclastic rock record: a summary of the diagnostic features. In: Eriksson, P.G., Altermann, W., Nelson, D.R., Mueller,

Schieber, J., Bose, P.K., Eriksson, P.G., Banerjee, S., Sarkar, S., Altermann, W., Catuneanu, O., 2007. Atlas of microbial mat features preserved within the siliciclastic rock record. Atlases in Geoscience 2. Elsevier, Amsterdam, p. 311.

Schieber, J., Southard, J.B., Schimmelmann, A., 2010. Lenticular shale fabrics resulting from intermittent erosion of water-rich muds—interpreting the rock record in the light of recent flume experiments. Journal of Sedimentary Research 80, 119-128.

Schumm, S.A., 1968. Speculations concerning paleohydraulic controls of terrestrial sedimentation. Geological Society of America Bulletin 79, 1573–1588.

Seilacher, A., 1982. Distinctive features of sandy tempestites. In., Einsele, G., Seilacher, A., (eds). Cyclic and event stratification (pp. 333-349). Springer Berlin Heidelberg.

Seilacher, A., 2007. Trace Fossil Analysis. Springer, Berlin, pp. 226.

Sheldon, N.D., 2012. Microbially induced sedimentary structures in the ca. 1100 Ma terrestrial midcontinent rift of North America. In., Chafetz, H. (eds). Microbial mats in siliciclastic depositional systems through time. SEPM Special Publication 101, 153-162.

Shepard, R.N., Sumner, D.Y., 2010. Undirected motility of filamentous cyanobacteria produces reticulate mats. Geobiology 8, 179–190.

Smith, D.G., 1976. Effect of vegetation on lateral migration of anastomosed channels of a glacier meltwater river. Geological Society of America Bulletin 87, 857-860.

Steiner, M., Reitner, J., 2001. Evidence of organic structures in Ediacara-type fossils and associated microbial mats. Geology 29, 1119-1122.

Sur, S., Schieber, J., Banerjee, S., 2006. Petrographic observations suggestive of microbial mats from Rampur Shale and Bijaigarh Shale, Vindhyan basin, India." Journal of earth system science 115, 61-66.

Sweet, I.P., 1988. Early Proterozoic stream deposits: braided or meandering—evidence from central Australia. Sedimentary geology 58, 277-293.

Tal, M., Paola, C., 2007. Dynamic single-thread channels maintained by the interaction of flow and vegetation. Geology 35, 347–350.

Thornes, J. B., 1990. Vegetation and erosion: processes and environments. Chichester: Wiley

1045 Tirsgaard, H., Øxnevad, I.E., 1998. Preservation of pre-vegetational mixed fluvio–aeolian deposits in a humid
1046 climatic setting: an example from the Middle Proterozoic Eriksfjord Formation, Southwest Greenland.
1047 Sedimentary Geology 120, 295-317.
1048
1049 Todd, S.P., Went, D.J., 1991. Lateral migration of sand-bed rivers: examples from the Devonian Glashabeg
1050 Formation, SW Ireland and the Cambrian Alderney Sandstone Formation, Channel Islands. Sedimentology 38,
1051 997-1020.
1052
1053 Tolhurst, T.J., Gust, G., Paterson, D.M., 2002. The influence of an extracellular polymeric substance (EPS) on
1054 cohesive sediment stability. In., Winterwerp, J.C., Kranenburg, C (eds). Fine Sediment Dynamics in the Marine
1055 Environment, pp. 409–426. Elsevier, Amsterdam.
1056
1057 Vandevivere, P., Baveye, P., 1992. Effect of bacterial extracellular polymers on the saturated hydraulic
1058 conductivity of sand columns. Applied and Environmental Microbiology 58, 1690–1698.
1059
1060 Vignaga, E., Sloan, D.M., Luo, X., Haynes, H., Phoenix, V.R., Sloan,W.T., 2013. Erosion of biofilm-bound
1061 fluvial sediments. Nat Geosci. 6, 770–774.
1062
1063 Wellman, C. H., Strother, P.K., 2015. The terrestrial biota prior to the origin of land plants (embryophytes): a
1064 review of the evidence. Palaeontology 58, 601-627.
1065
1066 Went, D.J., 2005. Pre-vegetation alluvial fan facies and processes: an example from the Cambro-Ordovician
1067 Rozel Conglomerate Formation, Jersey, Channel Islands. Sedimentology 52, 693-713.
1068
1069 Went, D.J., 2013. Quartzite development in early Palaeozoic nearshore marine environments. Sedimentology
1070 60, 1036-1058.
1071
1072 Went, D.J., Andrews, M.J., 1990. Post-Cadomian erosion, deposition and basin development in the Channel
1073 Islands and northern Brittany. In: D'Lemos, R.S., Strachan, R.A., Topley, C.G., (eds). The Cadomian Orogeny.
1074 Geological Society Special Publication 51, 293-304.

Went, D.J., Andrews, M.J., 1991. Alluvial fan, braided stream and possible marine shoreface deposits of the Lower Palaeozoic Erquy-Fréhel Group, northern Brittany. Proc. Ussher Soc. 7, 385-391).

Went, D.J., Andrews, M.J., Williams, B.P.J., 1988. Processes of alluvial fan sedimentation, basal rozel conglomerate formation, la têcte des hougues, Jersey, Channel Islands. Geological Journal *23*, 75-84.

Wilmeth, D.T., Dornbos, S.Q., Isbell, J.L., Czaja, A.D. 2014. Putative domal microbial structures in fluvial siliciclastic facies of the Mesoproterozoic (1.09 Ga) Copper Harbor Conglomerate, Upper Peninsula of Michigan, USA. Geobiology 12, 99-108.

Yeo, G.M., Percival, J.B., Jefferson, C.W., Ickert, R., Hunt, P., 2007. Environmental significance of oncoids and crypto-microbial laminates from the Late Paleoproterozoic Athabasca Group, Saskatchewan and Alberta. Bulletin-Geological Survey of Canada 588, 315.

1099

1100

1101

Typical Values	Pre-vegetated	Post-Vegetated	Reasons
Sand-body aspect ratio	Extremely High; Dominant sheet-braided architecture at normal outcrop scale	Highly Variable (e.g., Channeled-braided, Sheet-braided, Ribbon)	Vegetation decreases sediment erodibility and increases bank stabilization[1]
Number/% of Fms with >10% Mud content	11 occurrences (references in table caption)	37.5% of VS3, 50% of VS4, 85.7% of VS5, 94.1% of VS6[1]	Vegetation promotes the production and preservation of muds, with fines bypassing pre-vegetation systems through fluvial and aeolian transport[1]
Sand-body Petrology	Largely arkose and quartzarenite groups described	Quartzarenite, arkose and litharenite groups commonly described	Physical transport processes in pre-vegetation environments may have enabled the rapid transport of unweathered feldspar, resulting in common arkosic sandstones[1]
Grain size distribution	Almost entirely medium-coarse sand (or greater)	High range of grain-size commonly recorded	Vegetation can decrease the proportion of sediment transported as bedload[1]
Stratification type	Trough- and planar-cross and horizontal stratification common	Trough and planar cross-stratification, ripple cross-lamination and horizontal stratification common	Transverse and linguoid bedforms occur in a wide variety of both pre-vegetation and post-vegetation fluvial settings
Sandy-Bedforms	Abundant	Abundant	Fields and trains of individual bedforms occur across a variety of fluvial settings
Preserved channel-forms	Rare	Common	Frequent channel switching in pre-vegetation systems results in poor preservation
Low-sinuosity Elements (e.g., DA)	Fairly Common	Fairly Common	Low sinuous bar-complexes occur within major sand-bodies in both pre-vegetation and post-vegetation fluvial systems.
Heterogeneous lateral accretion sets	Unusual but present	Fairly Common	Expansion of rooted plants increased overall river sinuosity, although pre-vegetation alluvial networks still contained higher-sinuosity portions within predominantly low-sinuosity systems[1]
Heterolithic lateral accretion sets	One described example[2]	Fairly Common	Major expansion of meandering rivers as rooted plants stabilized river banks[1]
Palaeosols	Very rare	Common	Terrestrial vegetation is suggested to have promoted diversification and increased complexity of pedogenic deposits[1]
Coal/Charcoal	Absent	Present from Devonian	Coals became abundant after the evolution of plant arborescence[1]
Interpreted Fluvial Styles	Dominantly low-sinuosity, bed-load dominated systems	Extremely Variable	Vegetation alters mechanisms of fluvial flow and deposition[1]

Table 1. Characteristic sedimentary products of both pre-vegetation and post-vegetation alluvium: 1. Davies and Gibling, 2010. VS = Vegetation Stage; 2. Santos and Owen, 2016. Pre-vegetation formations with >10% mud content; Harrison, 1979; Germs, 1983; Sweet, 1988; Els, 1995; Kemp, 1996; Tirsgaard and Øxnevad, 1998; Driese et al., 2011; Köykkä, 2011; Marconato et al., 2014; Went, 2016.

Figure 1. (A) Location of Series Rouge 'Red Beds'. Numbered boxes indicate location of presented architectural panels: 1. Sables d'Or Quarry (Fig. 13); 2. Pointe aux Chèvres (Fig. 10); 3. Îlot Saint-Michel (Fig. 14)

Figure 2. Top: Lithostratigraphic correlation of formations constituting Series Rouge. Formations comprising Series Rouge boxed. Summaries of sedimentology presented in Section 4. Carteret Formation fauna from Doré, 1994. 1. Auvray, (1979); 2. Miller et al., (2001); 3. D'lemos et al., (2001); 4. Hagstrum et al., (1980); 5. Pasteels & Doré, (1982); 6. Auvray et al., 1980; 7. Pillola, 1993. *Saint-Jean-de-la-Rivière Formation. Bottom: Typical outcrops and interpreted environments for Series Rouge members

Figure 3. Petrographic evidence for matground colonisation in the Fréhel Formation; (A) Detrital biotite mica with approximately aligned long-axes (red arrow indicates wavy-crinkly morphology); (B) Pale green biotite with cleavage planes; (C-D) Wavy-crinkly morphology exhibited by detrital biotite mica (examples arrowed); (E) Fréhel Formation mudstone with interpreted carbonaceous stringers; (F) Differential compaction of carbonaceous stringers surrounding suspended quartz grain; (G) Petrographic thin section of mud clast hosting carbonaceous material present; (H) Delaminating oxidised biotite mica fraying towards its lateral margin

Figure 4. (A) Transverse wrinkles. Fréhel Formation. Diameter of coin is 24 mm; (B) Transverse wrinkles. Port Lazo Formation. Diameter of coin is 27 mm; (C) 'Bubble-texture'. Fréhel Formation; (D) Epirelief bulges. Fréhel Formation. Diameter of coin is 24 mm; (E) Ruptured domes. Port Lazo Formation; (F) Elephant skin texture. Port Lazo Formation; (G) Curved shrinkage cracks. Port Lazo Formation. Diameter of coin is 24 mm; (H) Reticulate markings (pimple structures to right of image associated with *Arumberia*-Fig. 6. Port Lazo Formation.

Figure 5. (A) *Aristophycus* structures. Fréhel Formation. Pen lid is 38 mm long; (B) Petrographic thin section of *Aristophycus*; (C) Petrographic thin section of sandstone horizon immediately adjacent to *Aristophycus*; (D) Petrographic thin section of sandstone horizon immediately underlying *Aristophycus*; (E) Vertical log of *Aristophycus* bearing section; (F) Schematic line of section across *Aristophycus.*

Figure 6. (A-B) *Arumberia* rugae. Diameter of coin is 21 mm; (C) Dimple-Pimple structures in association with *Arumberia*; (D) Carbonaceous material (arrowed) draped over mud laminae; (E) Petrographic thin section of drab mudstone hosting *Arumberia*, showing clearly deformed mud laminae and carbonaceous material. All images from Port Lazo Formation.

Figure 7. Vertical log through Fréhel Formation. Locations of presented architectural element analysis are indicated.

Figure 8. (A) Trough-cross stratification; (B) Conglomerate lying above down-flow dipping reactivation surface; (C) Example of downstream accretion macroform. Percentage values under rose indicate scale of external ring. Dashed lines indicate interpreted bar-form top and bottom surfaces. All Fréhel Formation.

136

137 **Figure 9.** Observed and interpreted architectural elements within this study (after Miall, 1985, 1996; Long, 2006).

138 **Figure 10.** (A) Architectural analysis of Fréhel Formation cropping out at Point aux Chévres. Successive sand-bodies identified
139 by number. The displayed data shows the relationship between set/co-set inclinations (red arrows) to their respective underlying
140 surfaces (strike-lines represented by blue barb). Accretion macroforms are mapped on in their exact lateral position within the
141 respective sandbody (horizontal scale). No vertical scale intended. Acronyms relate to inferred architectural element (Fig. 9).
142 Sandy-bedforms are not included in diagram; (B) Succession presented in (A); (C) Rose plots of sandbodies from (A). Blue
143 arrows show dip direction of genetically related surfaces (presented as strike-lines in (A)). Percentage values under rose diagrams
144 display circumference scale. Measurements: Palaeoflow $\theta = 116$; Bounding surfaces $\theta = 51$

145 **Figure 11.** (A) Proximal down-flow variations of accretion within individual bar-form. Person is 187 cm tall. Yellow lines denote
146 lower and upper surfaces of interpreted bar-form; (B) Example of a downstream-lateral accretion macroform. Person is 187 cm
147 tall; (C) Downstream accretion macroform; (D) Schematic diagram of prograding stack of downstream accreting macroforms; (E)
148 Trough-cross stratification. All images from Fréhel Formation, Series Rouge.

149 **Figure 12.** (A) Discontinuous sandstone body within along-strike section at Pointe aux Chèvre, Fréhel Formation. Metre rule for
150 scale; (B) Interpretative line drawing of 12A; (C) Thin mudstone layer highlighted in 12B. Compass-clinometer is 10.5 cm long;
151 (D) Petrographic thin section of mudstone in 12C, displaying wavy-crinkly laminae constituted by detrital mica.

152 **Figure 13.** Architecture of braided alluvium at Sables d'Or quarry. Panel demonstrates the high lateral continuity of sand-bodies.
153 Blue arrows represent palaeoflow orientations measured from cross-bed foresets. Blue pins represent dip directions of set/coset
154 boundaries. The directions indicated by the arrows and pins have been corrected for tectonic tilt, and are organized with respect to
155 the architectural panel so that arrows pointing up indicate dip directions away from the observer, and those pointing down indicate
156 dip directions towards the observer. Procedure after Long, 2006. Accretion macroforms annotated (in colour version, lines denote
157 accretion macroform type: Yellow, DA; Orange, DLA/iDLA; Pink, LA/iLA; Green, Channel; Black, SB/iSB)

158 **Figure 14.** Architectural panel at Îlot Saint-Michel. Note that lateral accretion surfaces adjacent to scale are directly measurable
159 and as such are labelled LA. Accretion macroforms higher in the cliff-face, such that measurements could not be obtained, are
160 given the prefix 'i' (see Section 4.1.1). Palaeoflow near directly out of cliff face.

161 **Figure 15**. Sparsely vegetated braidplain of the Mimer River, Spitsbergen (78° 39' 07" N, 16° 10' 47" E) as a partial modern
162 analogue to a pre-vegetation river, showing distribution of microbial features and their ineffectiveness in buffering against
163 physical processes. A) Incipient patches of young moss (examples arrowed) on a bar top, acting as loci for colonization by
164 cyanobacterial individuals of the genus Rivularia (inset). B) Recently emergent biofilm on drying margin of shallow bar-top

drainage channel, showing bubble formation in EPS (black arrow) and sediment cavities arising from gas expulsion by respiring microbiota (white arrow). C) Biological soil crust, also colonized by tracheophytes, on the margin of an active trunk channel. Undercutting of soil crust by fluvial channel is apparent (white arrow) and clasts of soil crust have become unroofed (black arrow), maintaining their integrity due to binding by tracheophyte roots. Note absence of evidence for microbiota in fast flowing, sediment-laden water of the main channel. D) Biofilm in sluggish lotic water of small bar-top drainage channel. Note that biofilm does not adhere to the substrate as a mat, and that the fastest flowing water has carved a passage through the biofilm along its thalweg (arrowed in direction of water flow).

Figure 16. Schematic reconstruction of relationships between: 1) Matgrounds and unvegetated river channels; 2) Embryophytes and other higher land plants and river channel

174

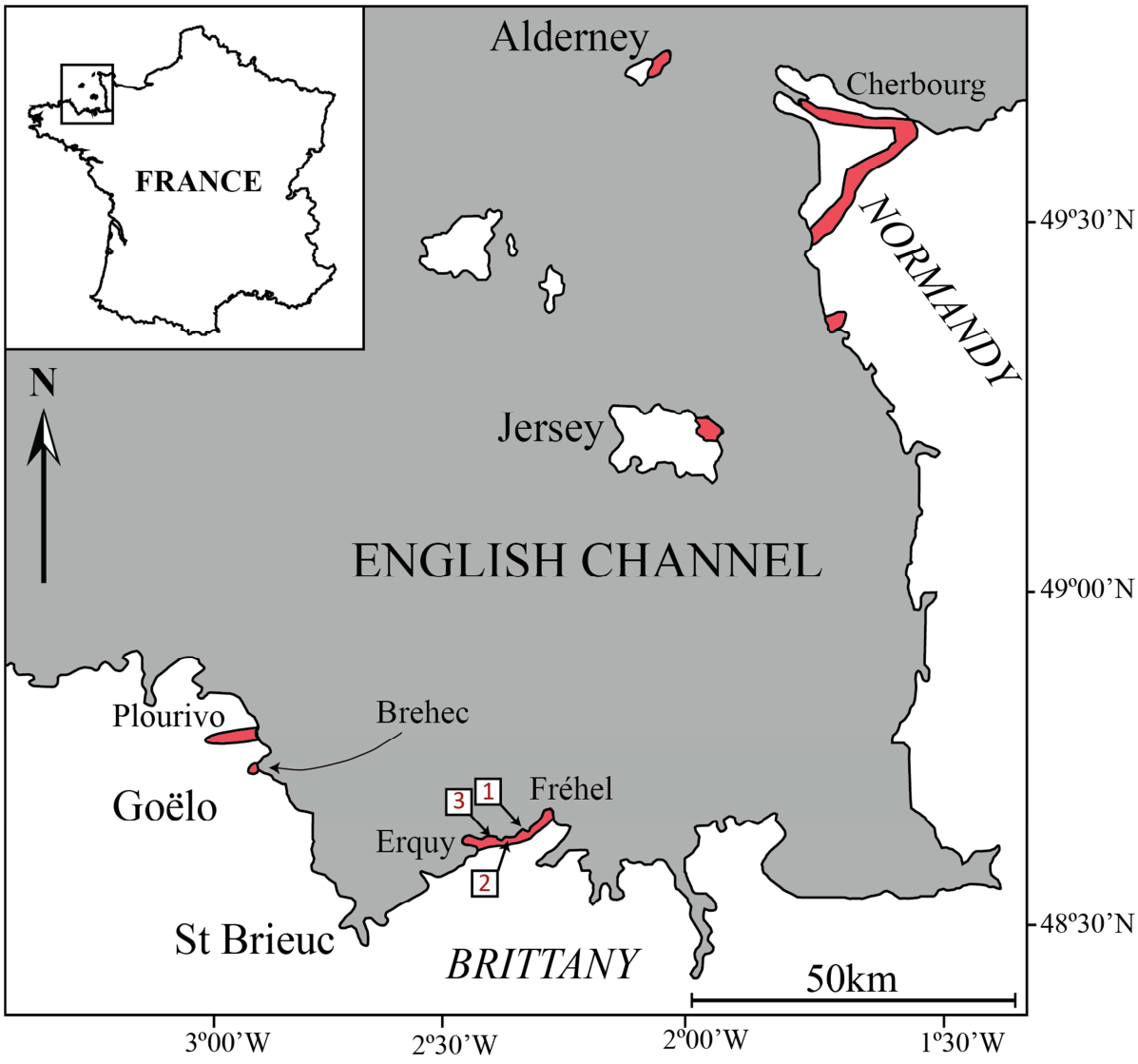
Alderney
Cherbourg
FRANCE
NORMANDY
49°30'N
N
Jersey
ENGLISH CHANNEL
49°00'N
Plourivo
Brehec
Goëlo
3
1
Fréhel
Erquy
2
St Brieuc
BRITTANY
50km
48°30'N
3°00'W
2°30'W
2°00'W
1°30'W

Fig. 1

Fig. 2

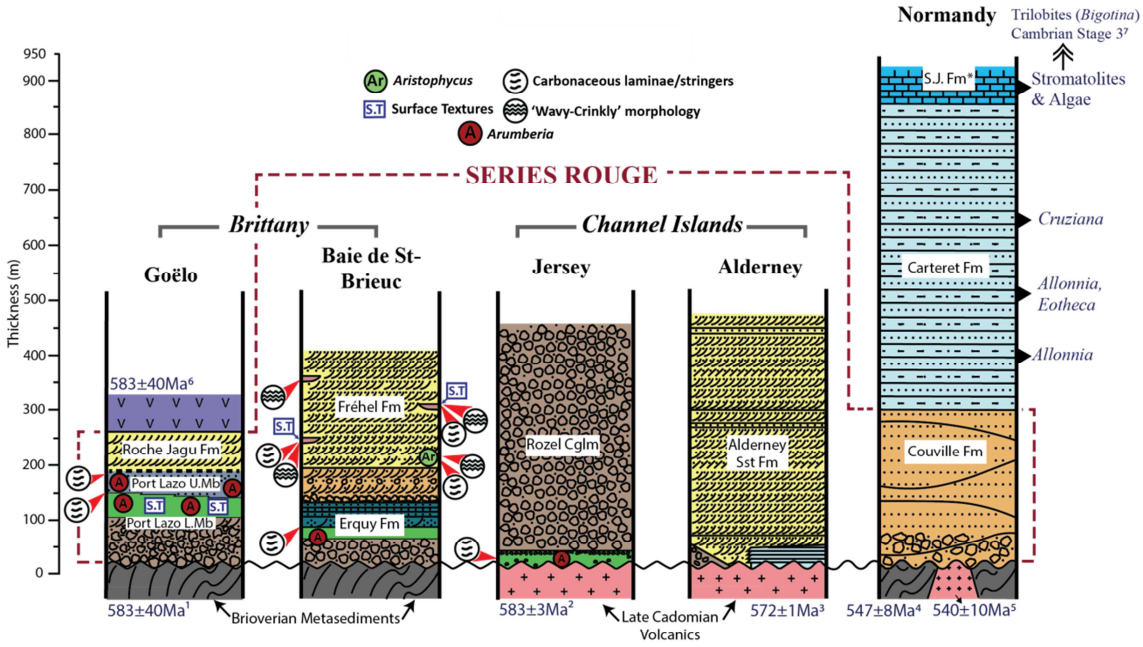

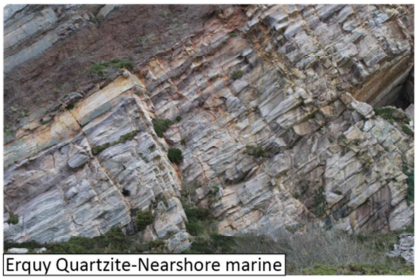
Erquy Quartzite-Nearshore marine


Alderney Sst Fm-Braided alluvial


Port Lazo Upper Mb-Subtidal


Rozel Cglm-Alluvial Fan

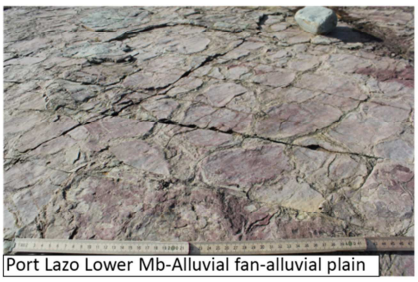
Port Lazo Lower Mb-Alluvial fan-alluvial plain


Fréhel Fm-Braided alluvial

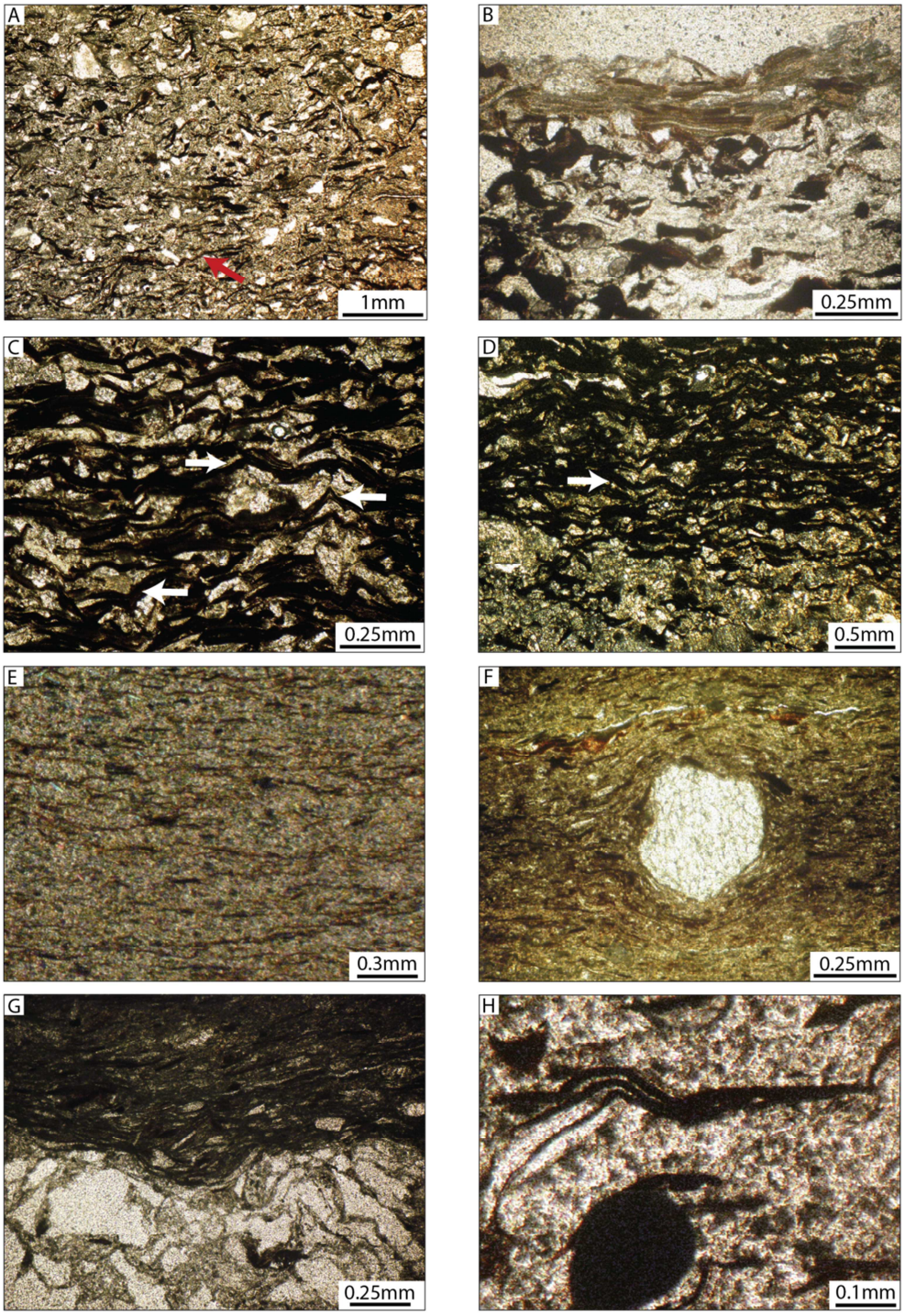

Fig. 3

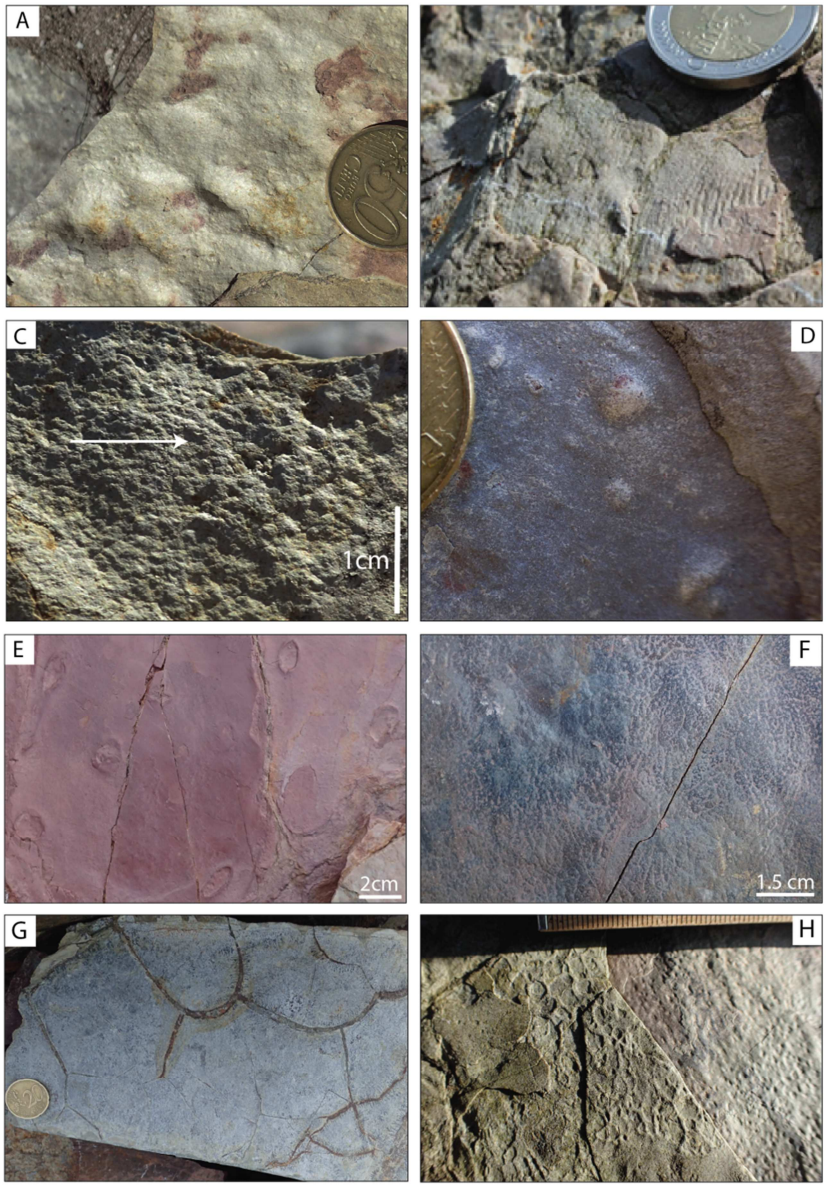

Fig. 4

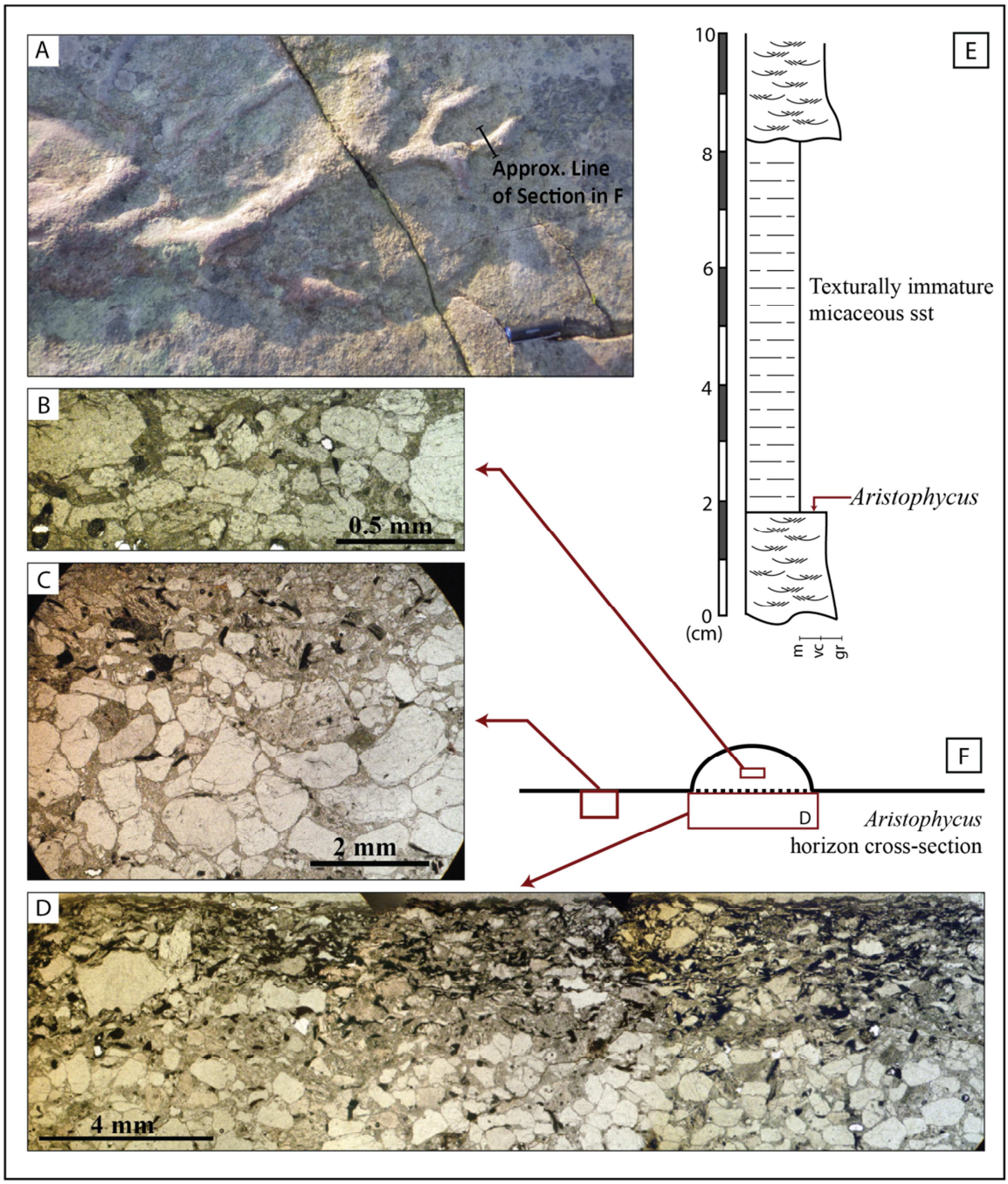
A
Approx. Line
of Section in F
B
0.5 mm
C
2 mm
D
4 mm
E
10
8
6
4
2
0
(cm)
Texturally immature
micaceous sst
Aristophycus
m
vc
gr
F
D
Aristophycus
horizon cross-section

Fig. 5

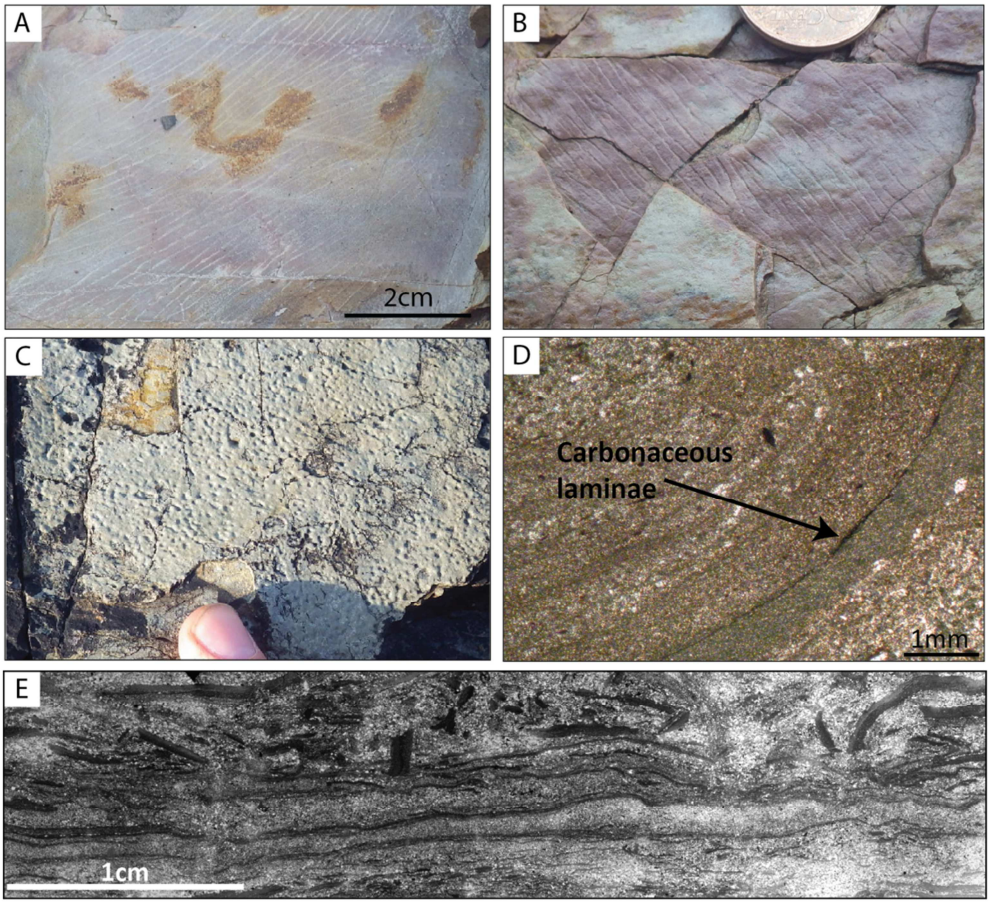

Fig. 6

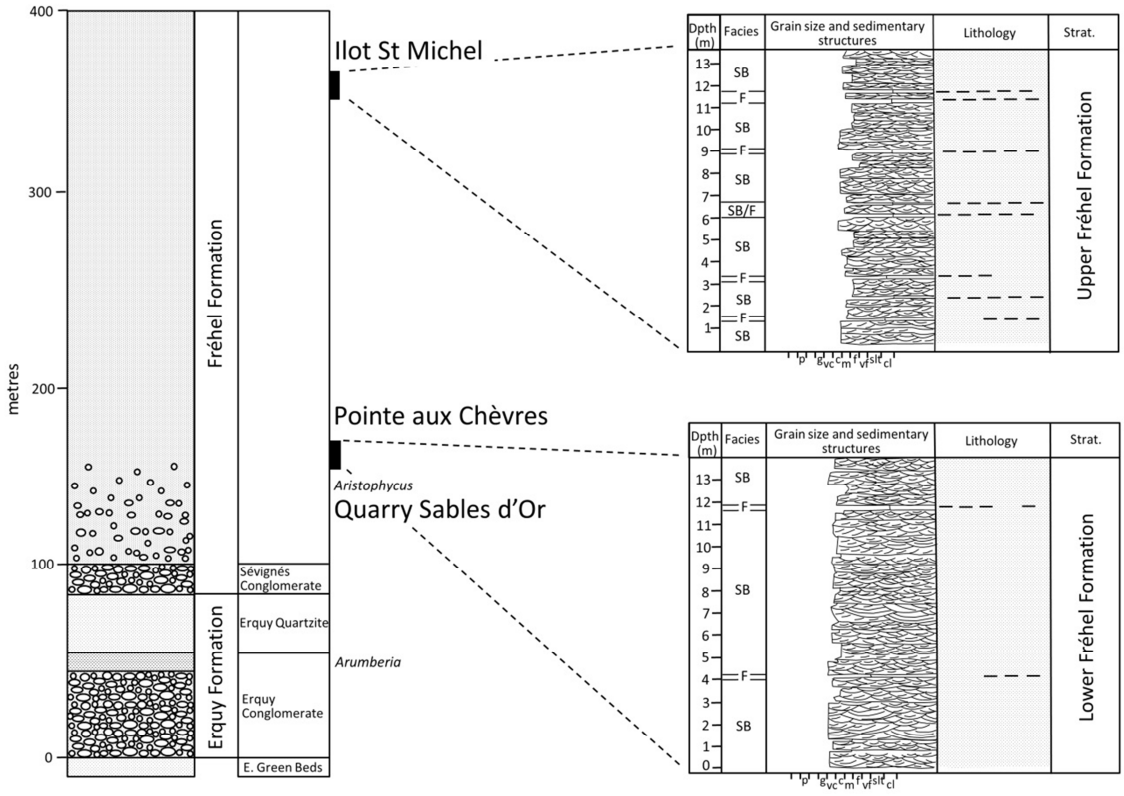
metres
400
300
200
100
0
Fréhel Formation
Erquy Formation
Sévignés Conglomerate
Erquy Quartzite
Erquy Conglomerate
E. Green Beds
Ilot St Michel
Pointe aux Chèvres
Aristophycus
Quarry Sables d'Or
Arumberia
Dpth (m)
Facies
Grain size and sedimentary structures
Lithology
Strat.
SB
F
SB/F
Upper Fréhel Formation
Lower Fréhel Formation
p
vc
c
m
vf
si
cl

Fig. 7

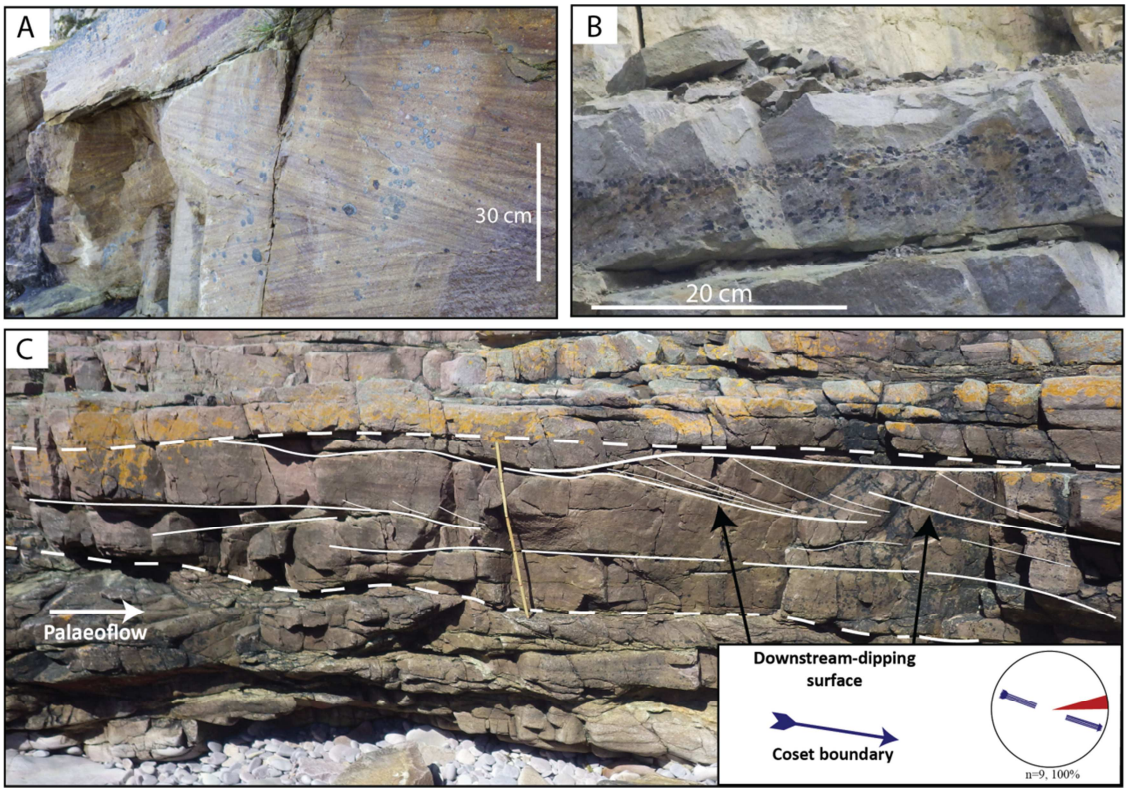
A
30 cm
B
20 cm
C
Palaeoflow
Downstream-dipping surface
Coset boundary
n=9, 100%

Fig. 8

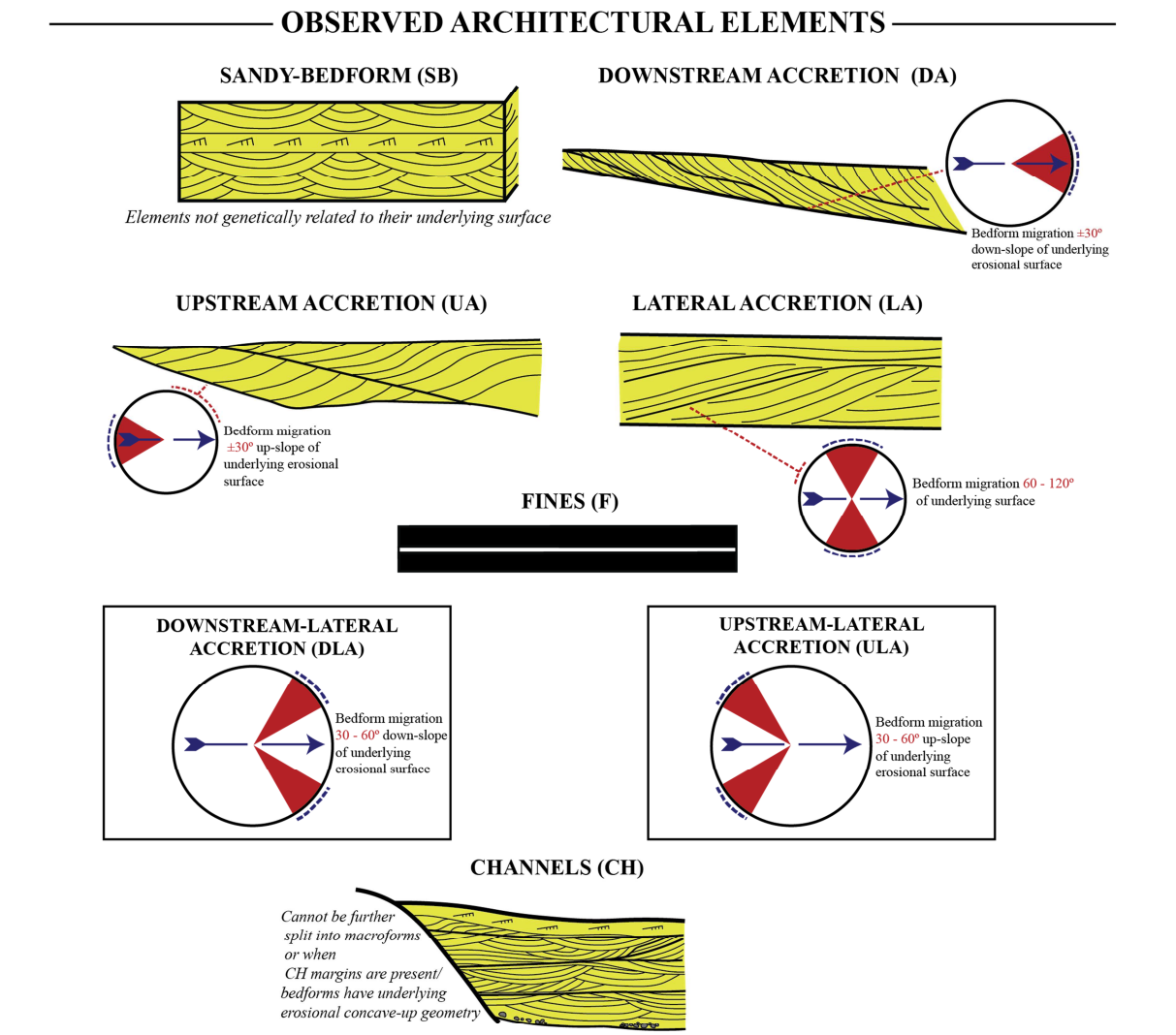
OBSERVED ARCHITECTURAL ELEMENTS
SANDY-BEDFORM (SB)
Elements not genetically related to their underlying surface
DOWNSTREAM ACCRETION (DA)
Bedform migration ±30° down-slope of underlying erosional surface
UPSTREAM ACCRETION (UA)
Bedform migration ±30° up-slope of underlying erosional surface
LATERAL ACCRETION (LA)
Bedform migration 60 - 120° of underlying surface
FINES (F)
DOWNSTREAM-LATERAL ACCRETION (DLA)
Bedform migration 30 - 60° down-slope of underlying erosional surface
UPSTREAM-LATERAL ACCRETION (ULA)
Bedform migration 30 - 60° up-slope of underlying erosional surface
CHANNELS (CH)
Cannot be further split into macroforms or when CH margins are present/ bedforms have underlying erosional concave-up geometry

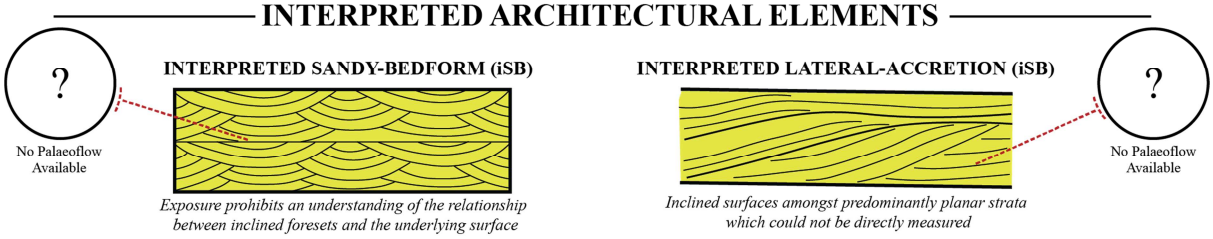
INTERPRETED ARCHITECTURAL ELEMENTS
?
No Palaeoflow Available
INTERPRETED SANDY-BEDFORM (iSB)
Exposure prohibits an understanding of the relationship between inclined foresets and the underlying surface
INTERPRETED LATERAL-ACCRETION (iSB)
Inclined surfaces amongst predominantly planar strata which could not be directly measured
?
No Palaeoflow Available

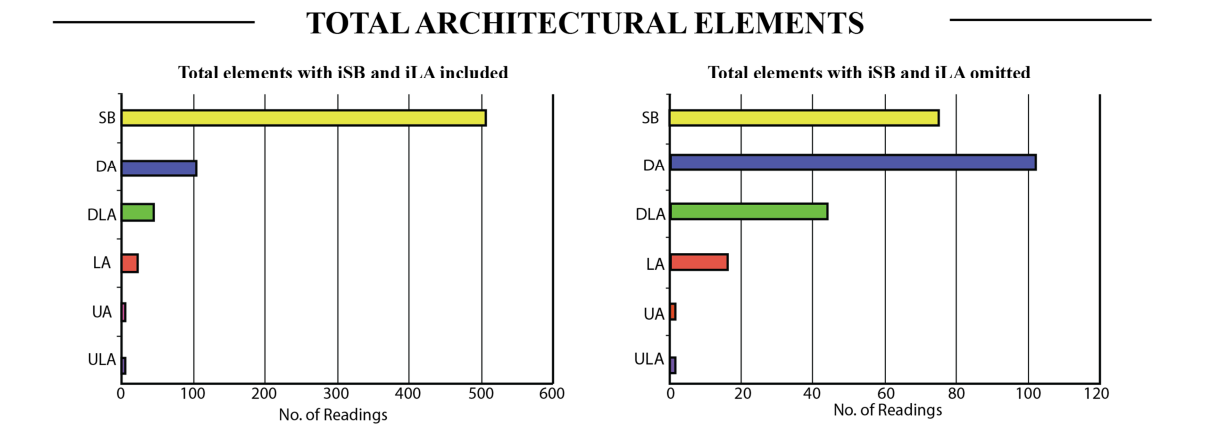
TOTAL ARCHITECTURAL ELEMENTS
Total elements with iSB and iLA included
SB
DA
DLA
LA
UA
ULA
0
100
200
300
400
500
600
No. of Readings
Total elements with iSB and iLA omitted
SB
DA
DLA
LA
UA
ULA
0
20
40
60
80
100
120
No. of Readings

Fig. 9

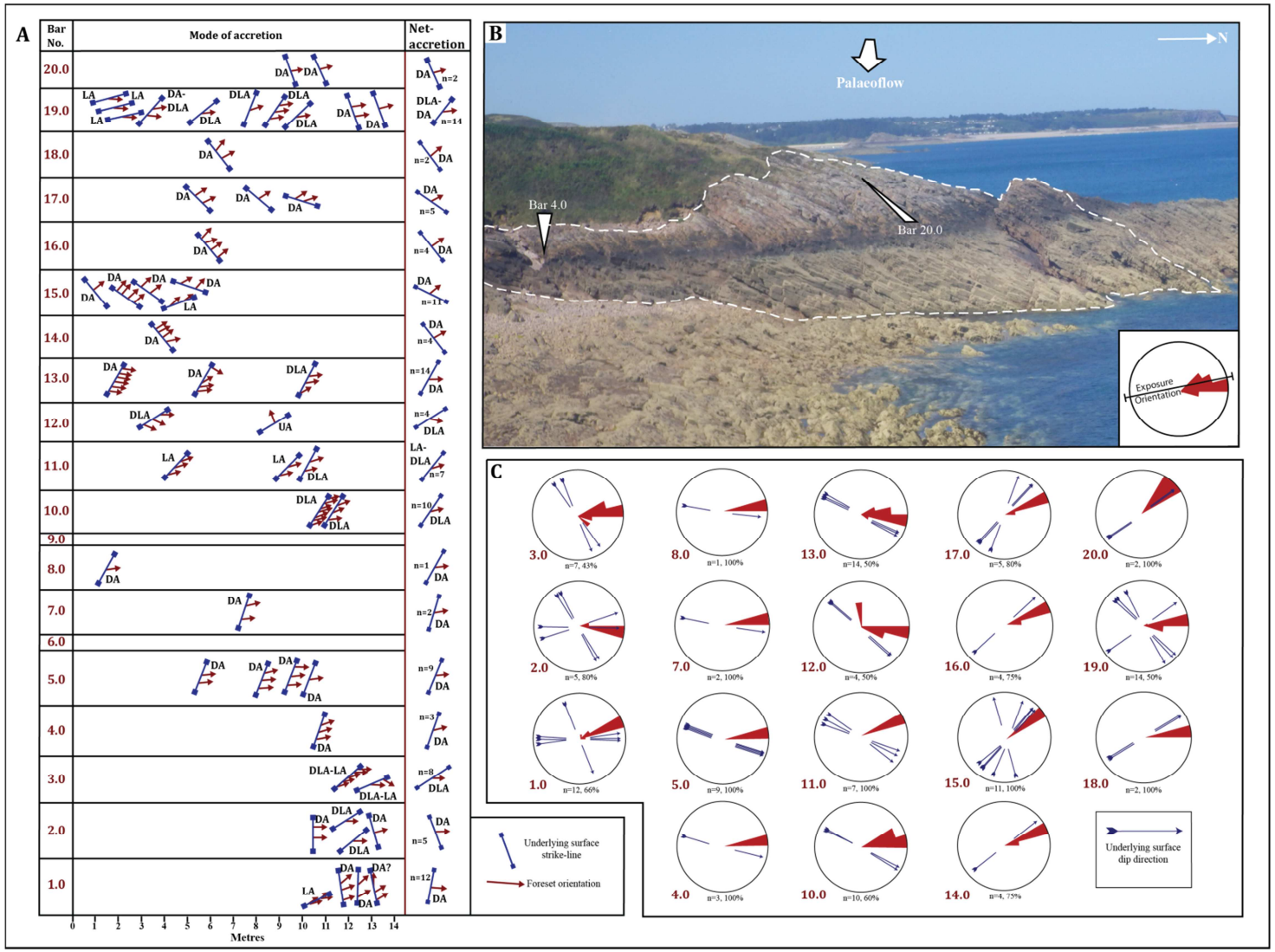
A
Bar No.
Mode of accretion
Net-accretion
20.0
19.0
18.0
17.0
16.0
15.0
14.0
13.0
12.0
11.0
10.0
9.0
8.0
7.0
6.0
5.0
4.0
3.0
2.0
1.0
0 1 2 3 4 5 6 7 8 9 10 11 12 13 14
Metres
B
Palaeoflow
N
Bar 4.0
Bar 20.0
Exposure Orientation
C
3.0 n=7, 43%
8.0 n=1, 100%
13.0 n=14, 50%
17.0 n=5, 80%
20.0 n=2, 100%
2.0 n=5, 80%
7.0 n=2, 100%
12.0 n=4, 50%
16.0 n=4, 75%
19.0 n=14, 50%
1.0 n=12, 66%
5.0 n=9, 100%
11.0 n=7, 100%
15.0 n=11, 100%
18.0 n=2, 100%
4.0 n=3, 100%
10.0 n=10, 60%
14.0 n=4, 75%
Underlying surface strike-line
Foreset orientation
Underlying surface dip direction

Fig. 10

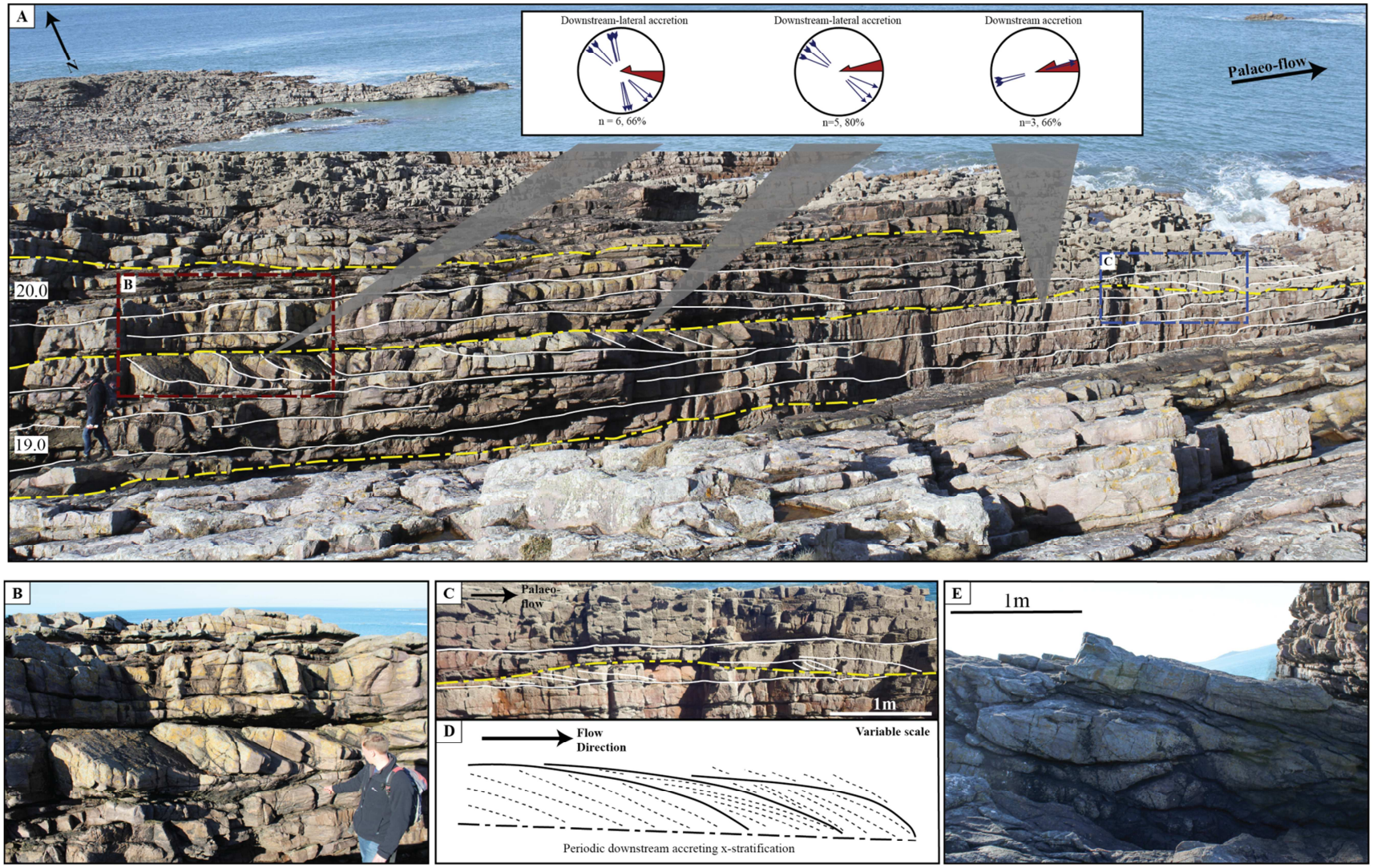
A
Downstream-lateral accretion
n = 6, 66%
Downstream-lateral accretion
n=5, 80%
Downstream accretion
n=3, 66%
Palaeo-flow
20.0
19.0
B
C
B
C
Palaeo-flow
1m
D
Flow Direction
Variable scale
Periodic downstream accreting x-stratification
E
1m

Fig.11

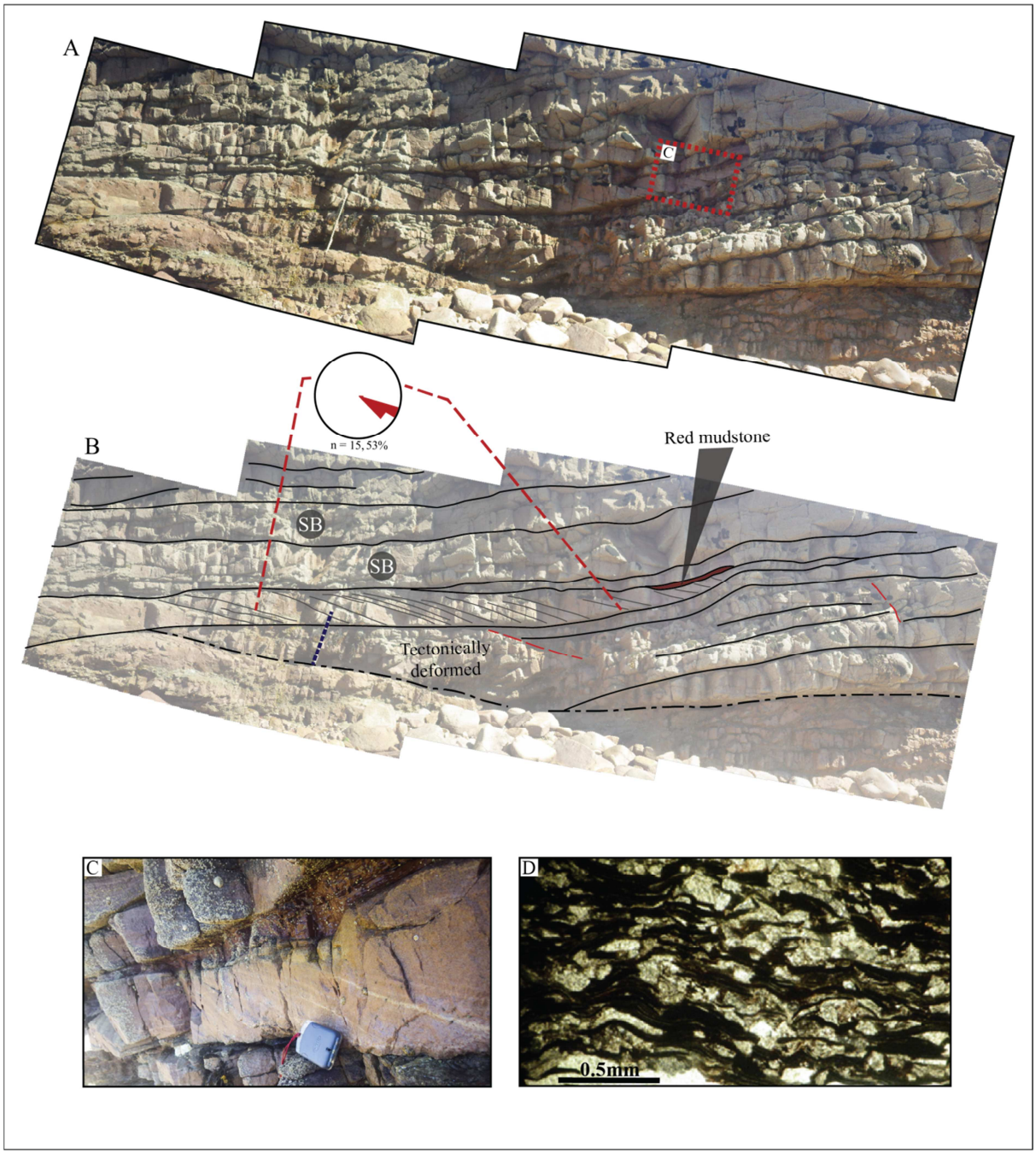

Fig. 12

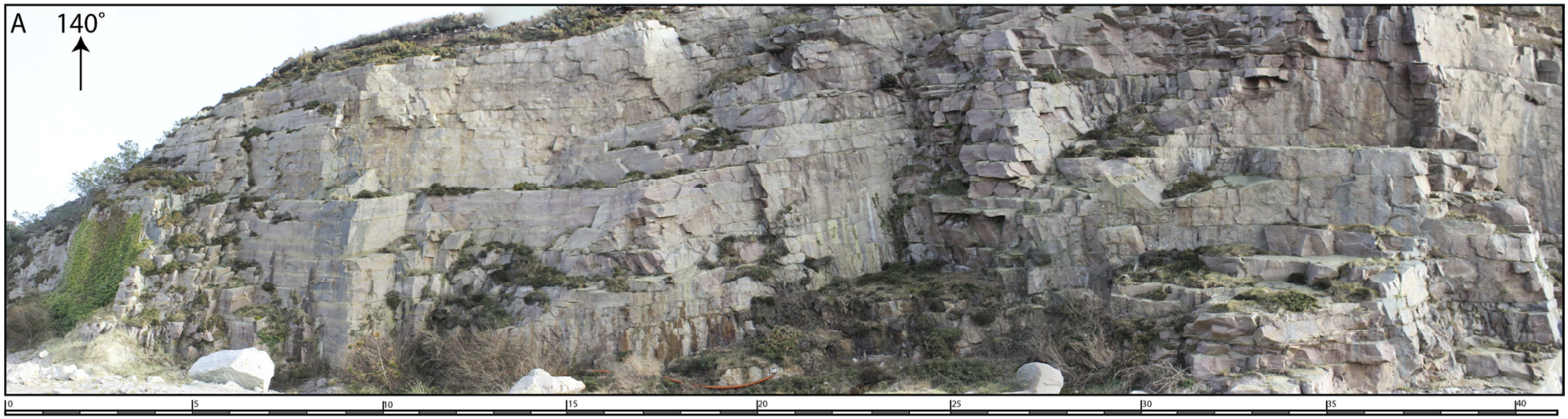
A
140°
0
5
10
15
20
25
30
35
40
Metres

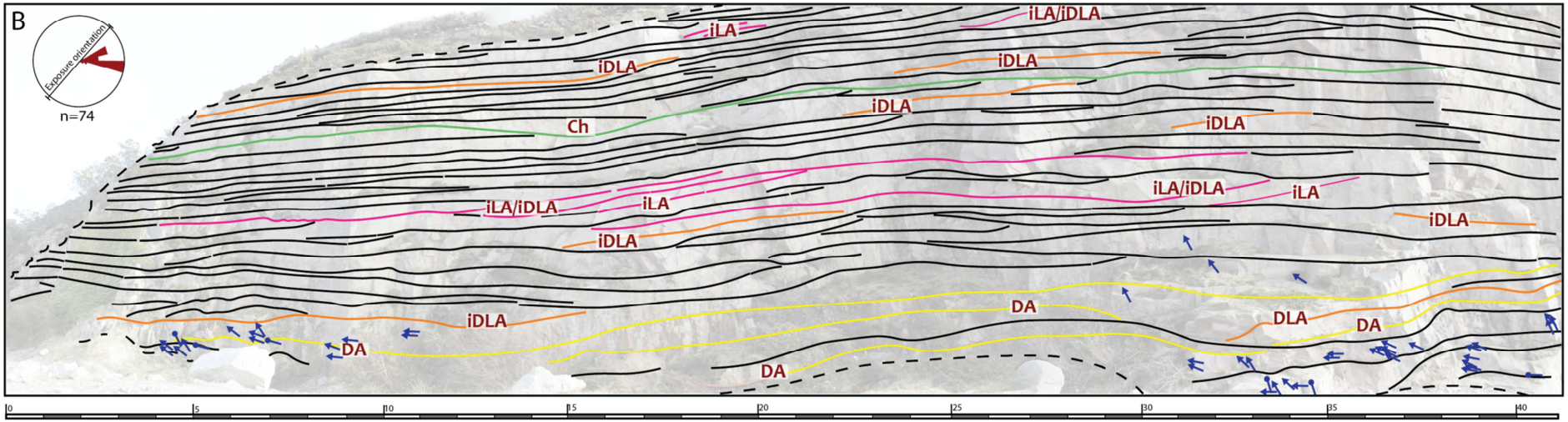
B
Exposure orientation
n=74
iLA
iDLA
Ch
iLA/iDLA
DA
DLA
0
5
10
15
20
25
30
35
40
Metres

F13

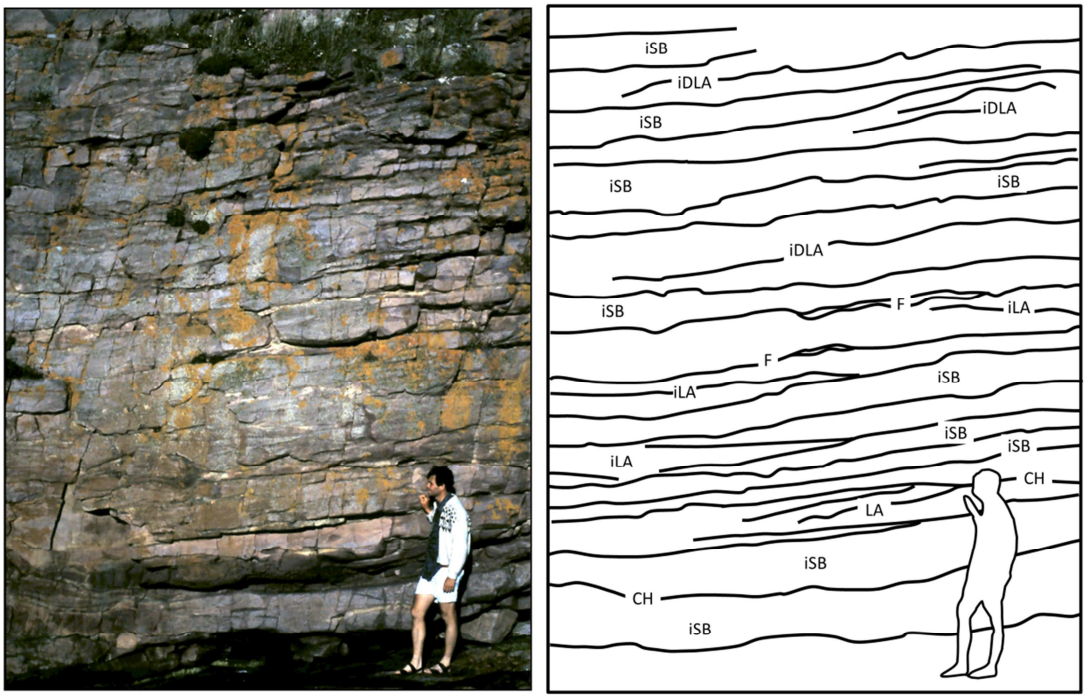
iSB
iDLA
iSB
iDLA
iSB
iSB
iDLA
iSB
F
iLA
F
iLA
iSB
iSB
iSB
iLA
CH
LA
iSB
CH
iSB

F14

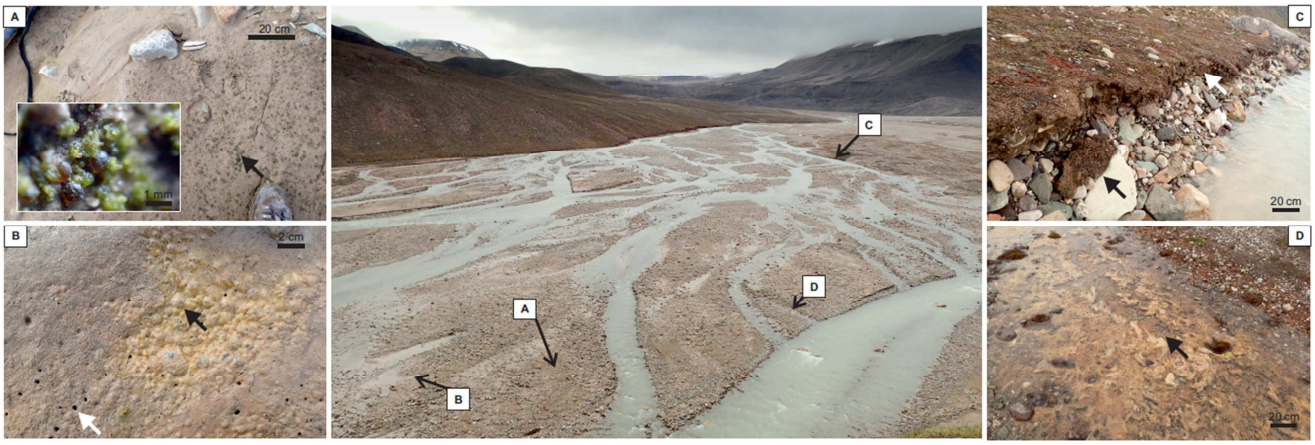
A
20 cm
1 mm
B
2 cm
C
A
B
D
C
20 cm
D
20 cm

F15

Fig. 16

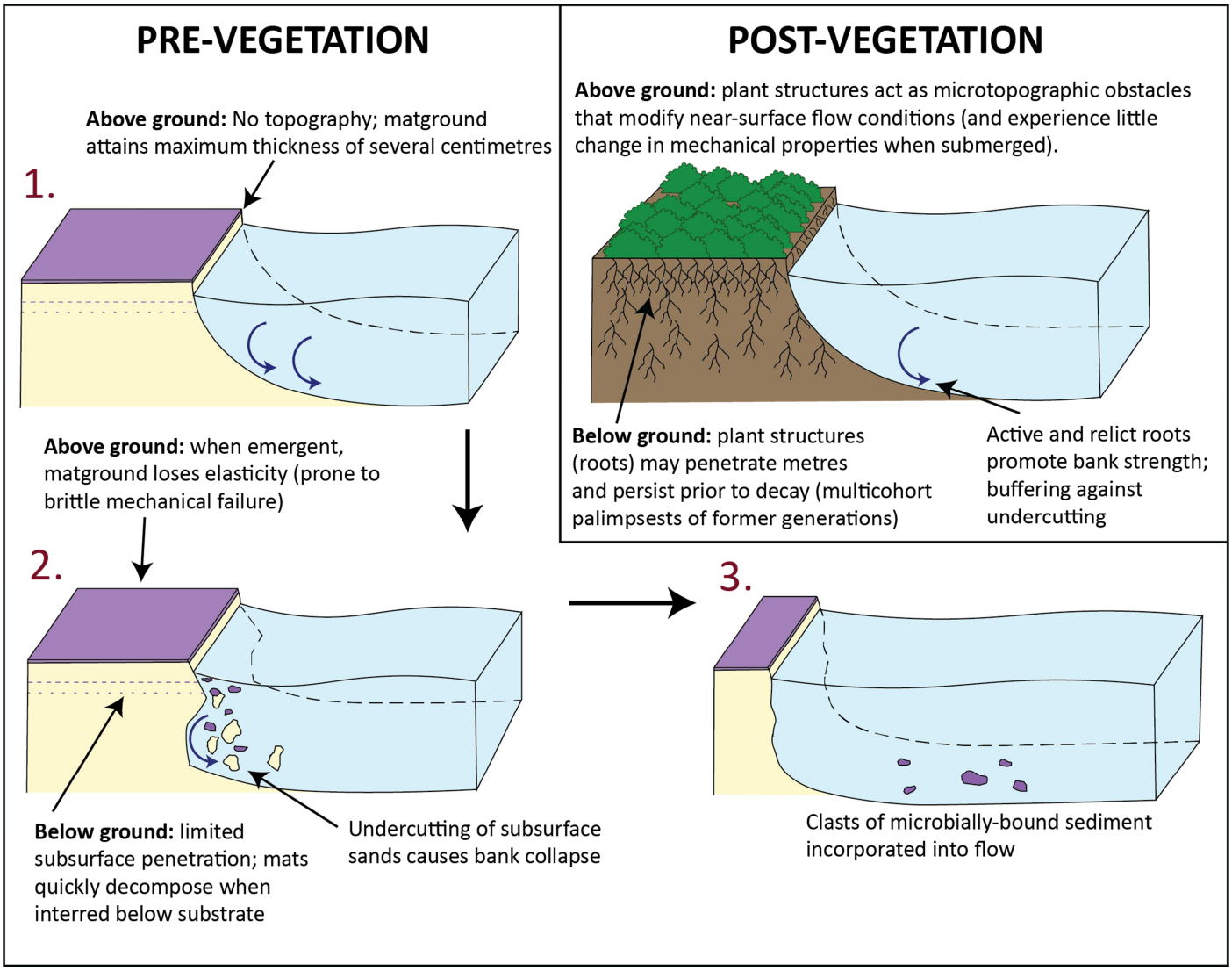
PRE-VEGETATION
POST-VEGETATION
Above ground: No topography; matground attains maximum thickness of several centimetres
1.
Above ground: plant structures act as microtopographic obstacles that modify near-surface flow conditions (and experience little change in mechanical properties when submerged).
Below ground: plant structures (roots) may penetrate metres and persist prior to decay (multicohort palimpsests of former generations)
Active and relict roots promote bank strength; buffering against undercutting
Above ground: when emergent, matground loses elasticity (prone to brittle mechanical failure)
2.
3.
Below ground: limited subsurface penetration; mats quickly decompose when interred below substrate
Undercutting of subsurface sands causes bank collapse
Clasts of microbially-bound sediment incorporated into flow